The Plant Cell, Vol. 15, 2430–2447, October 2003, www.plantcell.org © 2003 American Society of Plant Biologists

Deletion Derivatives of the *MuDR* Regulatory Transposon of Maize Encode Antisense Transcripts but Are Not Dominant-Negative Regulators of Mutator Activities

Soo-Hwan Kim[1,2] and Virginia Walbot

Department of Biological Sciences, Stanford University, Stanford, California 94305-5020

The maize *MuDR*/*Mu* transposable elements are highly aggressive, and their activities are held in check by host developmental and epigenetic mechanisms. The Mutator regulatory element, *MuDR*, produces both sense and antisense transcripts. We have investigated the impact of the presence of antisense transcripts on the abundance of the corresponding sense messages and on the regulation of Mutator activities. We report that internal deletions in *MuDR* arise frequently in somatic tissues; preferential loss of the 3′ untranslated region of *mudrA* and/or *mudrB* containing the intergenic region is correlated with chimeric sense *mudrA*/antisense *mudrB* and sense *mudrB*/antisense *mudrA* transcripts. Heritable internal deletions are extremely frequent ($>10^{-2}$ per element), and the resulting defective *MuDR* elements also encode antisense transcripts. Expression of endogenous or additional transgene-encoded antisense transcripts neither decreases sense transcript levels nor inhibits Mutator excision activity over the three generations examined. We propose that antisense transcripts produced by *MuDR* deletions are not dominant-negative regulators of Mutator activities.

INTRODUCTION

MuDR/*Mu* transposable elements of maize are extremely active in transposition, increasing mutation frequency by 50- to 100-fold above the spontaneous level (Walbot, 1992). *MuDR* elements in active Mutator plants encode functional MURA transposase (Eisen et al., 1994) and a MURB helper protein (Lisch et al., 1999) that excise diverse, multicopy *MuDR*/*Mu* elements and insert them into new loci throughout the maize genome (reviewed by Walbot and Rudenko, 2002).

One host control of Mutator activities is that *MuDR*/*Mu* transposition is restricted to cells undergoing the terminal cell divisions of tissue development, minimizing sector size and the number of gametes with each new mutation (Levy and Walbot, 1990; Raizada and Walbot, 2000; Raizada et al., 2001c). A counter strategy is that *MuDR*/*Mu* switches from "cut-and-paste" excision and insertion in the soma to a "replicative" outcome in the germinal cells and gametophytes. Therefore, *Mu* elements increase in copy number (Walbot and Rudenko, 2002). A second host control is that epigenetic loss of Mutator activity is very common (Walbot, 1986; Martienssen and Baron, 1994). The initiation of silencing coincides with the nuclear retention of nonpolyadenylated RNA derived from *MuDR* and *MuDR* homologs (*hMuDR* elements) (Rudenko et al., 2003). Epigenetic silencing is correlated with the methylation of the terminal inverted repeats (TIRs) (Chandler and Walbot, 1986) and the absence of *MuDR* transcripts (Hershberger et al., 1991).

[1] Current address: Department of Plant Biology, Carnegie Institution of Washington, Stanford University, Stanford, CA 94305.

[2] To whom correspondence should be addressed. E-mail soohwan@andrew2.stanford.edu; fax 650-325-6857.

Article, publication date, and citation information can be found at www.plantcell.org/cgi/doi/10.1105/tpc.014605.

Multiple levels of regulation have been proposed to explain the complex developmental and epigenetic regulation of Mutator activities. Both *MuDR* genes, *mudrA* and *mudrB*, encode alternatively spliced transcripts. Hence, it is possible that different MURA and MURB proteins program specific components of Mutator activities (Hershberger et al., 1995). Other mechanisms proposed to downregulate Mutator activities or maintain the silenced status include post-translational modifications of MURA or MURB (Walbot and Rudenko, 2002), poison proteins encoded by the homologs of *MuDR* (Rudenko and Walbot, 2001), host proteins that interfere with MURA binding to the TIRs until late in development (Benito and Walbot, 1997; Raizada et al., 2001b), developmentally progressive retention of *MuDR*/*hMuDR* RNA inside of the nucleus (Walbot and Rudenko, 2002), expression of the *Mop1* gene (Lisch et al., 2002), introduction of a dominant silencing factor, *MuKiller* (Lisch, 2002), and the balance of sense and antisense *MuDR* transcripts (Hershberger et al., 1995; Lisch et al., 1999).

Antisense transgenes are used routinely to eliminate or reduce endogenous gene expression in plants (Bourque, 1995). Antisense RNAs are hypothesized to exert negative regulation by annealing to their complementary sense transcripts. The resulting double-stranded RNA structure may directly affect mRNA maturation, transport to the cytoplasm, RNA stability, or translation (Terryn and Rouze, 2000). Alternatively, double-stranded RNA can trigger small RNA–mediated post-transcriptional gene silencing (reviewed by Waterhouse et al., 2001). In some cases, antisense RNAs encode small proteins (Knee et al., 1997), and some of these serve as signal molecules (Bisseling, 1999).

There are several cases in which antisense RNAs are negative regulators of transposons. For example, *Escherichia coli Tn10* transposon is inhibited by element-encoded antisense RNA, which interferes with translation by pairing with the 5′ end of the

transposase mRNA (Simons and Kleckner, 1988). The *micropia* retrotransposon in *Drosophila hydei* encodes a testis-specific antisense RNA complementary to the reverse transcriptase and RNase H coding regions. This antisense transcript is hypothesized to control the germ line expression of the corresponding sense transcripts (Lankenau et al., 1994).

mudrA and *mudrB* are transcribed convergently from promoters in the TIRs, and their polyadenylation sites are separated by only a 225-bp intergenic region composed of numerous short repetitive elements (Figure 1A) (Hershberger et al., 1995). Recently characterized *hMuDR* elements are transcriptionally active but produce messages with numerous nucleotide polymorphisms, and these elements cannot program Mutator activities (Rudenko and Walbot, 2001). In active Mutator plants, RNase protection assays identified sense transcripts as well as antisense transcripts that are collinear with the *MuDR* genes (Hershberger et al., 1995). As determined by in situ hybridization, antisense *mudrA* transcripts colocalized with sense *mudrA* and *mudrB* transcripts, whereas antisense *mudrB* transcripts were difficult to detect in most tissues (Joanin et al., 1997). Interestingly, the detection of all *MuDR* transcripts by in situ hybridization increased significantly when RNA was denatured before hybridization. This finding suggests that the sense and antisense transcripts may have been paired in vivo.

Diverse antisense *MuDR* transcript types have been characterized in this study. We propose that somatic deletions within *MuDR* elements generate derivatives that encode substantial and diverse chimeric transcripts. These chimeric constructs consist of sense *mudrA* and antisense *mudrB* or sense *mudrB* and antisense *mudrA* and presumably resulted from the failure of transcription termination within the intergenic region. Molecular and genetic analysis of heritable *MuDR* deletions producing antisense transcripts and of transgenic maize expressing specific forms of antisense RNA demonstrated that neither endogenous nor transgene-encoded antisense transcripts affect the levels of *MuDR* sense transcripts or *Mu* excision activity over three generations. Although these results do not prove that Mutator is inherently insensitive to antisense RNA, they do indicate that Mutator activities are tolerant of the types and levels of antisense transcripts produced by somatic and germinal deletion derivatives, both of which arise at a high frequency in active Mutator lines. Therefore, the possibility that these antisense *MuDR* transcripts are immediate and effective negative regulators of Mutator activities is excluded by this study.

RESULTS

Cloning and Characterization of Somatic Antisense *MuDR* Transcripts

As determined by RNA gel blot analysis using single-stranded RNA or double-stranded DNA probes to detect *MuDR* transcripts in a survey of 65 plants, we found that most active Mutator plants produce transcripts with a mixture of discrete sizes plus a background smear; a subset of transcripts is antisense (data not shown). One plant was examined in detail to identify the origin of antisense transcripts. As shown in lane 1 of Figure 1B, the active Mutator plant SK26-1 contains multiple, intact 4.9-kb *MuDR* elements as well as a heritable, unmethylated 1.2-kb *MuDR* deletion derivative (*ΔMuDR*). RNA gel blot hybridizations demonstrate that this Mutator plant expressed not only the expected 2.8-kb *mudrA* (lane 2) and 1.0-kb *mudrB* (lane 3) transcripts encoded by intact *MuDR* elements but also three smaller transcripts detected by a double-stranded *mudrA* probe (lane 2). These short transcripts could be either sense or antisense transcripts. We did not detect a full-length "read-through" transcript of 4.7 kb that would represent full-length sense *mudrA*/antisense *mudrB* or sense *mudrB*/antisense *mudrA* transcripts.

Reverse transcription (RT) PCR was tested as an alternative to recover individual chimeric sense/antisense transcripts using total RNA isolated from a seedling leaf of SK26-1 (Figure 1C). Chimeric transcripts (sense *mudrB*/antisense *mudrA*) of varying lengths were amplified using primer 11 as the RT primer and primer 2 as the PCR amplification primer (Figure 1C, lane 1, Table 1). The amplification products were not derived from DNA templates, because no products were amplified when the RNA preparation was pretreated with RNase (Figure 1C, lane 2). Also, different product sizes were obtained when primer 2 was used as the RT primer (Figure 1C, lane 3) to amplify sense *mudrA*/antisense *mudrB* transcripts. We found both polyadenylated (Figure 1C, lane 4) and nonpolyadenylated (Figure 1C, lane 5) antisense *mudrB*/sense *mudrA* transcripts. Supporting evidence for the existence of poly(A)-tailed antisense *mudrB* transcripts was obtained by DNA sequence analysis of RT-PCR fragments amplified using a poly(dT)-anchored adaptor primer and an antisense *mudrB*-specific primer. Interestingly, one type of polyadenylated antisense *mudrB* cDNA had several single–base pair mismatches and an insertion of a nonhomologous DNA fragment, implying that this transcript originated from a *hMuDR* element (Figure 2).

Using several primer sets complementary to different regions of *mudrA* or *mudrB*, 13 chimeric sense/antisense transcripts of diverse lengths were retrieved and sequenced (Table 1). Most transcripts were unique; 12 transcripts were found only once, and 1 transcript (case 5) was retrieved multiple times. One sequence (case 1) was completely collinear with *MuDR* throughout its length of 517 bp. By contrast, 12 of 13 of the antisense transcripts were collinear with only portions of *MuDR*; each transcript was missing one or two different segments of *MuDR* (7 bp in case 4A up to 2909 bp in case 4B). Three transcripts (cases 3 through 5) were missing two segments of *MuDR*, one within the intergenic region and one within a gene (Table 1). These missing segments could result from RNA splicing or from the transcription of deleted templates. Sequence inspection indicated that the borders of the missing segments did not match even relaxed consensus splice sites (Brendel et al., 1998). In a previous study, four *mudrA* transcripts lacking internal segments were inferred to arise from *ΔMuDR* rather than from RNA splicing (Hershberger et al., 1995). Although the intergenic region is only 225 bp (positions 3301 to 3525) of the 4.9-kb *MuDR* element, 10 antisense transcript types were missing all (cases 3, 4, 5, 7, 8, 11, and 12) or a portion (cases 2, 6, and 10) of the intergenic region. As determined by gel blot analysis, the source plant SK26-1 had only one detectable truncated *MuDR* element and only three detectable short *mudrA* transcripts (Figure 1B). Therefore, we infer that most chimeric an-

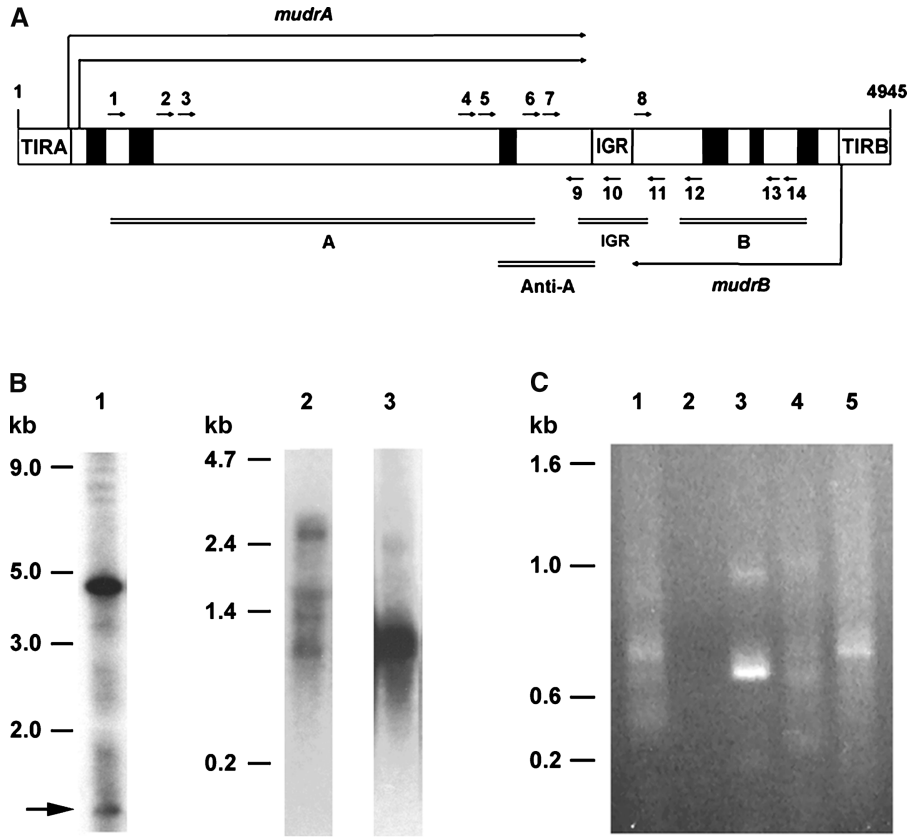

Figure 1. RT-PCR Amplification and Characterization of Somatic Antisense *MuDR* Transcripts from a Standard Mutator Plant Carrying Multicopy *MuDR* Elements.

(A) Scheme of the 4.9-kb *MuDR* element, which encodes two genes (*mudrA* and *mudrB*) that are transcribed convergently from the TIRA and TIRB promoters. An AT- and repeat-rich intergenic region (IGR) separates these genes (Hershberger et al., 1995). Closed boxes represent introns, and open boxes indicate exons. The positions and directions (5′ to 3′) of the RT-PCR primers used in this study are shown by short arrows. Each primer has a number corresponding to the 5′ base according to Hershberger et al. (1991), and A, B, or IGR at the beginning of each primer name indicates that the primer resides within *mudrA*, *mudrB*, or the intergenic region, respectively: 1, A493; 2, A1621; 3, A1813; 4, A2298; 5, A2713; 6, A2907; 7, A2952; 8, IGR3501; 9, A3276; 10, IGR3469; 11, B3843; 12, B3950; 13, B4334; and 14, B4473. *MuDR* regions recognized by hybridization probes are indicated by double lines and labeled as follows: A for a probe detecting *mudrA*; B for a probe detecting *mudrB*; Anti-A for a region of *mudrA* used for the generation of antisense *mudrA* transgenic plants; and IGR for the intergenic region.

(B) Heritable *MuDR* derivatives in the standard Mutator plant SK26-1 and characterization of *MuDR* transcripts. DNA gel blots prepared with SstI-digested DNA were probed with a DNA fragment that detects both *mudrA* and *mudrB* (A and B) as shown in **(A)**. The band of 4.7 kb represents an intact, unmethylated *MuDR* element. *MuDR* fragments >4.7 kb are methylated elements and/or *hMuDR* elements that lack the SstI site in the TIRs (Rudenko and Walbot, 2001). Bands <4.7 kb indicate deleted *MuDR* derivatives and are marked with an arrow (lane 1). In lanes 2 and 3, total RNA was extracted from the same SK26-1 plant, and RNA gel blots were hybridized with double-stranded *mudrA* (A) or *mudrB* (B) probes to detect *mudrA* and/or antisense *mudrA* (lane 2) or *mudrB* and/or antisense *mudrB* (lane 3).

(C) RT-PCR amplification of antisense *MuDR* transcripts from RNA fractions (see Methods) extracted from plant SK26-1. Different sizes of chimeric *mudrA*/antisense *mudrB* transcripts were amplified using an antisense *mudrB*-specific primer (primer 11 in **[A]**) for RT, followed by an amplification of the cDNA with primer 2 (lanes 1, 2, 4, and 5). In lane 2, RNA was pretreated with RNase A before reverse transcription. In lane 3, primer 2 was used as the RT primer and primer 11 was used for cDNA amplification. Total (lanes 1, 2, and 3), poly(A^+) (lane 4), or poly(A^-) (lane 5) preparation was used for the RT-PCR analysis. Forty cycles of PCR amplification were used. PCR products were fractionated on a 1% agarose gel and stained with ethidium bromide.

tisense transcripts are encoded by diverse somatic (substoichiometric) *ΔMuDR* elements.

Using transient expression experiments, fragments of *MuDR* were examined for promoter activity that could result in an antisense transcript of one gene with or without chimeric continuation to the sense transcript of the other gene. Schemes of the antisense promoter constructs are shown in Figure 3, and transient analysis data are presented in Table 2. Weak promoter activities that could result in sense *mudrA*/antisense *mudrB* transcripts were detected in constructs harboring the distal half of *mudrA* and the intergenic region (*pBP2*; ~10.1% of the control TIRB promoter activity derived from *pMB5*) and the intergenic region

Table 1. Sequence Analysis of Antisense *MuDR* Transcripts Recovered from a Leaf Patch of SK26-1

Primer Sets[a]	Transcript Type[b]	Case Number[c]	Deletion (bp) [Position][d]	Flanking Sequence at the Deletion End Points[e]	Insertion (bp) [Position][f]
7/10	B and αA	1		None	None
		2	98 [3344 to 3441]	TTATTTCagttttatt—gcaattgtCGCCCAG	None
7/14	B and αA	3A	963 [3189 to 4151]	GTATTTGttgtaaga—agtttagaTGCCTCC	None
		3B	72 [4226 to 4297]	AAGATCCtgtgcaa—atccatacCACATTC	None
11/1	A and αB	4A	7 [612 to 618]	TTAGttgtaagACTG	None
		4B	2909 [743 to 3651]	ATTATAGtatcagat—aacaaacACTACGG	2 [743]
		5A	86 [595 to 680]	AGTTGGAagactgct—acattgtcTGTAATA	None
		5B	2303 [1252 to 3554]	TTGGGTCgcattcca—acactgagCCATTAG	289 [1252]
11/2	A and αB	6	1562 [1928 to 3489]	GTATTTGaacaccat—gaaatagaGCGCAGA	None
		7	1771 [1964 to 3734]	TTCACAAgattgctg—caaaatgaGACACCA	17 [1964]
		8	1193 [2608 to 3800]	TCTCGAGggtgggag—ggtcgtttATCTCTT	30 [2608]
		9	1370 [1912 to 3281]	GGCCTATaggagaga—cagtgtatTTGTTGT	None
11/6	A and αB	10	441 [3090 to 3530]	CTAGTGAagaaaatc—gataacatATAACAC	17 [3090]
		11	554 [3171 to 3724]	TGTGCTCagaacaac—atcccagaCAGACCA	None
14/6	A and αB	12	1180 [3155 to 4334]	GCTAAGAacaaccac—ccttctccACGGCAA	None
		13	805 [3033 to 3837]	GCCGATGaaccagcc—gatagtgcTCTTCGA	27 [3033]

[a] RT primer/PCR amplification primer. See Figure 1A for the positions and directions of primers.
[b] Chimeric transcript of *mudrB* (B) and antisense *mudrA* (αA) or *mudrA* (A) and antisense *mudrB* (αB).
[c] Individual RT-PCR products were amplified using the primer set listed in the first column. Three RT-PCR products (cases 3, 4, and 5) have two deletions in each cDNA, and these deletions are noted as items A and B.
[d] Length of the missing *MuDR* sequence for each RT-PCR product. The 5′ to 3′ positions indicated in brackets are based on *MuDR* numbering according to Hershberger et al. (1991).
[e] Sequences of flanking deletion end points, expressed as 5′ to 3′. The bases extending to each side of the deletions are shown in uppercase letters. Missing *MuDR* sequences are shown in either lowercase letters or dashes when deleted nucleotides are not shown. A direct repeat of 3 bp near the junction is underlined.
[f] Length of filler DNAs in base pairs and their positions relative to *MuDR*.

itself (*pBP4*; ~15.1% of the TIRB activity). No significant promoter activity was detected in other coding regions in either reading frame. These results, considered together with the structures of the antisense transcripts, suggest that it is termination failure rather than internal antisense promoters that result in chimeric transcripts. *ΔMuDR* elements lacking the intergenic region appear to permit read-through transcription of *mudrA* or *mudrB* messages initiated from the TIR promoters.

Characterization of Heritable Genomic Deletions

In addition to somatic deletions, numerous heritable *MuDR* deletions have been reported (Hsia and Schnable, 1996; Lisch et al., 1999); however, the frequency of such deletions has not been quantified. We crossed active Mutator plants to and by standard maize anthocyanin tester lines lacking *MuDR*. Twelve families of progeny were examined for *MuDR* copy number and for the presence of deletions in *MuDR* elements (Table 3). SstI-digested genomic DNA was probed with a mixture of *mudrA* and *mudrB* fragments to identify deleted *MuDR* and then reprobed with the intergenic region DNA fragment to determine which of the already identified deleted elements were missing this specific region. Altogether, we found 20 newly arisen *ΔMuDR* elements plus 22 parental deletion derivatives segregating in the progeny. Some newly arisen derivatives found in several progeny plants represented a tassel sector in a parental plant that allowed transmission to multiple individuals.

Strikingly, 21 of the 42 analyzed deletions (50%) and 8 of 20 new deletions (40%) removed the 3′ untranslated region (UTR) of *mudrA* and/or *mudrB* containing the intergenic region, as determined by the failure to detect cross-hybridization with the 250-bp intergenic region probe. The deletion frequency was exceptionally high; considering just the singular deletions, events occurred in 18.9% of the plants in one generation (20 deletions in 106 plants). Most plants carry 5 to 20 copies of *MuDR* elements (copy number reconstruction data not shown); thus, these internal deletions occur at a frequency of 9.4×10^{-3} to 3.8×10^{-2} per element; 20 new deletions arose from an estimated 530 to 2120 copies of *MuDR* elements in 106 plants. Because very short deletions could have been overlooked, we consider our data to be minimal estimates of *ΔMuDR* production.

Structure and Transcript Types of Two Heritable *ΔMuDR* Elements

To evaluate the impact of antisense messages transcribed from germinally transmittable *ΔMuDR* derivatives, we characterized two specific *ΔMuDR* derivatives and their transcripts. DNA gel blot analysis of 11 sibling Mutator plants, SB03-1 to SB03-11, showed that this family has four *ΔMuDR* derivatives: three deletions (*ΔMuDR1*, *-3*, and *-4*) were transmitted to all siblings, and *ΔMuDR2* was segregating in the family (Figure 4A). Based on an analysis of progenitors, we determined that *ΔMuDR1* was generated during the growth of the great grandparent of the SB03 plants and became homozygous after self-pollination, whereas

```
MuDR     AACCATTTCCCATAGCTCTGGATCTTCTGTACTGTA  CCCATCACCAAGTTCATCA
cDNA#1   AACCATTTCCCATAGCTCTGGATCTTCTGTACTGTA  CCCATCACCAAGTTCATCA
cDNA#2   AACCATTTCCCATAGCTCTGGATCTTCTGTACTGTA  CCCATCACCAAGTTCATCA
cDNA#3   AACCATTTCGCATAGTTCTGGATCTTTTGTACTGTAAACCCCATCACCAAGTTCATCA
cDNA#4   AACCATTTCCCATAGNTCTGGATCTTCTGTACTGTA  CCCATCACCAAGTTCATCA

MuDR     TCATCTAGAGGATGTTCATCATCTACGGAAGGGTTGTCGTAAAGATCCCAAGTTGGA
cDNA#1   TCATCTAGAGGATGTTCATCATCTACGGAAGGGTTGTCGTAAAGATCCCAAGTTGGA
cDNA#2   TCATCTAGAGGATGTTCATCATCTACGGAAGGGTTGTCGTAAAGATCCCAAGTTGGA
cDNA#3   TCATCTAGAGGATGTTCATCATCTACGGAAGGGTTGTCGTAAAGATCCCAAGTTGGA
cDNA#4   TCATCTAGAGGATGTTCATCATCTACGGAAGGGTTGTCGTAAAGATCCCAAGTTGGA

MuDR     TTCTTAGTTTCTAAATCTTCTTCACAGATACTTGAAGTTTTGTCTAGCTCCTTGCAC
cDNA#1   TTCTTAGTTTCTAAATCTTCTTCACAGATACTTGAAGTTTTGTCTAGCTCCTTGCAC
cDNA#2   TTCTTAGTTTCTAAATCTTCTTCACAGATACTTGAAGTTTTGTCTAGCTCCTTGCAC
cDNA#3   TTCTTAGTTTCTAAATCTTCTTCACAGATACTTGAAGTTTTGTCTAGCTCCTTGCAC
cDNA#4   TTCTTAGTTTCTAAATCTTCTTCACAGATACTAAAAAAAAAAAAAAAAAAAA
                                      *4030

MuDR     ACATGTTCCAGAAACCCGCGAACCTTACCTATCTTGCCACCTTGTACCTCTGGAATA
cDNA#1   ACATGTTCCAGAAACCCGCGAACCTTACCTATCTTGCCACCTTGTACCTCTGGAATA
cDNA#2   ACATGTTCCAGAAACCCGCGAACCTTACCTATCTTGCCACCTTGTACCTCTGGAATA
cDNA#3   ACATGTTCCAGAAACCCGCGAACCTTACCTATCTTGCCACCTTGTACCTCTGGAATA
cDNA#4

MuDR     GTCGAACACAATTTTTGAACCGAATGCAACAGTTTAGATTGCCTCCTCATTTCTTGA
cDNA#1   GTCGAACACAATTTTTGAACCGAATGCAACAGTTTAGATTGCCTCCTCATTTCTTGA
cDNA#2   GTCGAACACAATTTTTGAACCGAATGCAACAGTTTAGATTGCCTCCTCATTTCTTGA
cDNA#3   GTCGAACACAATTTTTGAACCGAATGCAACAGTTTAGATTGCCTCCTCAAAAAAAAA
cDNA#4
                                                        *4150

MuDR     ATAGCATATCTCAACGAAATTCTTTATGCTCACATGATACTTGAAGTCGACAAGATC
cDNA#1   ATAGCATATCTCAACGAAATTCTTTAAAAAAAAAAAAAAAAAAAA
cDNA#2   AAAAAAAAAAAAAAAAAA
cDNA#3   AAAAAAAAAAAA
cDNA#4
         *4159                    *4193
```

Figure 2. Nucleotide Alignment of Polyadenylated Antisense *mudrB* Transcripts Along with the Corresponding *MuDR* Sequence.

A two-nucleotide insertion and three single nucleotide mismatches in cDNA#3 are shown in boldface and italic type, respectively. The stars indicate polyadenylation starts, and the numbers represent their positions according to *MuDR* numbering for each antisense cDNA (Hershberger et al., 1991). All cDNA fragments were retrieved multiple times.

ΔMuDR2 was produced in a grandparent (data not shown). Using PCR, we amplified and sequenced regions surrounding the deletion junctions of *ΔMuDR1* and *ΔMuDR2*. Figure 4B shows simplified schemes. *ΔMuDR1* has an intact *mudrB* gene but lacks 1136 bp (positions 2350 to 3485). Consequently, a segment spanning the 3′ coding region and the 3′ UTR of *mudrA* as well as most of the intergenic region are missing. *ΔMuDR2* is missing 1568 bp (positions 2158 to 3725), including part of *mudrB*, all of the intergenic region, and ~40% of *mudrA*. The 1.0 kb of *ΔMuDR1* and 0.57 kb of *ΔMuDR2* sequence examined were perfectly collinear with *MuDR* except for these deletions.

Directional RT-PCR was performed to distinguish transcripts initiating in TIRA from those initiating in TIRB of *ΔMuDR1* and *ΔMuDR2*. Based on its intact *mudrB* structure, we expected chimeric sense *mudrA*/antisense *mudrB* and *mudrB* transcripts from *ΔMuDR1*. However, both *mudrA*/antisense *mudrB* and *mudrB*/antisense *mudrA* transcripts were amplified from this deletion derivative (Figure 4C, lanes 1, 2, 5, and 6). Similarly, Lisch et al. (1999) found that deletion of just 174 bp from the 3′ end of *mudrA* resulted in the termination failure of *mudrB*. Therefore, it appears that a DNA structure in the 3′ UTR of *mudrA* or in the intergenic region is important for the successful termination of *mudrB* transcription. *ΔMuDR2* also produced both antisense *mudrA* and antisense *mudrB* read-through transcripts, as expected, because both genes lack a 3′ UTR and the intergenic region is missing (Figure 4C, lanes 2, 3, 6, and 7). As determined by sequencing, the amplified RT-PCR fragments were shown to be identical to the corresponding deletion derivative (data not shown). No novel splicing events were observed in either *ΔMuDR1* or *ΔMuDR2* transcripts. Interestingly, the majority of chimeric transcripts from both deletion derivatives lacked polyadenylation (Figure 4D, lanes 2 and 5), suggesting that the chimeric transcripts may be retained in the nucleus. As a control, the majority of actin transcripts were polyadenylated, suggesting that they are cytoplasmic mRNA (Figure 4D, lane 9).

Epigenetic Regulation of *ΔMuDR* Transcript Abundance and Lack of Measurable Impact on *mudrA* Transcript Level and *Mu1* TIR Methylation

With confirmation that heritable deletion derivatives are transcriptionally active, we next examined the relative abundance of sense and chimeric antisense transcripts. RT-PCR was used to simultaneously amplify antisense *mudrA* and antisense *mudrB* transcripts (Figure 4E, top two gels) of *ΔMuDR1* and/or *ΔMuDR2*.

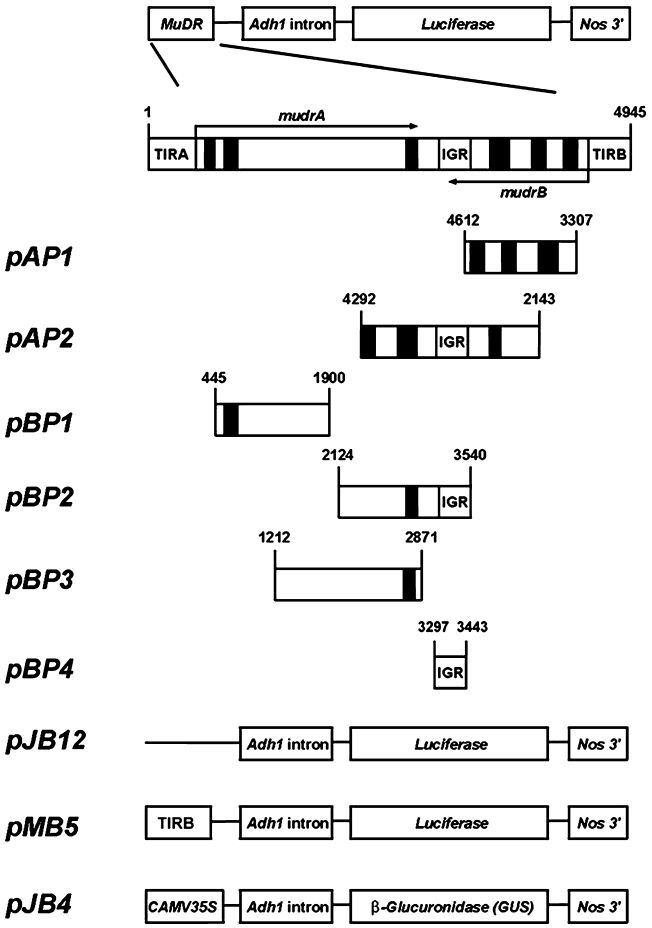

Figure 3. Schemes of the Constructs Used in Experiments Testing Antisense Promoter Activities.

Numbers on each scheme indicate the positions in *MuDR*. Drawings are not to scale. *CaMV*, *Cauliflower mosaic virus*; *Nos*, nopaline synthase.

Table 2. Transient Analysis for Antisense Promoter Activity of Different *MuDR* Regions in Maize Black Mexican Sweet Protoplasts

Promoter Constructs[a]	Luciferase Expression[b]
Antisense *mudrA* activity	
pAP1 [4612 to 3307]	88 ± 18
pAP2 [4292 to 2143]	75 ± 13
Antisense *mudrB* activity	
pBP1 [445 to 1900]	58 ± 16
pBP2 [2124 to 3540]	185 ± 21
pBP3 [1212 to 2871]	62 ± 15
pBP4 [3297 to 3443]	275 ± 18
Expression control	
pJB12	32 ± 8.5
pMB5	1823 ± 160

[a] Schemes of the constructs used in this experiment are shown in Figure 3. The *Cauliflower mosaic virus* 35S promoter region of a luciferase expression construct, *pJD312*, was replaced with a region of *MuDR* fragment. The 5′ to 3′ positions of the *MuDR* fragment fused to the expression cassette are indicated in brackets. *pJB12* (*pJD312* without the *Cauliflower mosaic virus* 35S promoter) was used as a negative control, and *pMB5* (TIRB:*Adh1* intron:*LUC*) was used as a positive control.
[b] Luciferase expression was normalized using GUS activity derived from *pJB4* as described in Methods.

From the same RNA preparation, the sense *mudrA* transcripts of an intact *MuDR* also were amplified (Figure 4E, third gel from the top). Interestingly, the expression of either *Δmudr1* and/or *Δmudr2* antisense transcripts did not significantly reduce the relative abundance of *mudrA* in 9 of 11 plants examined. Additionally, *Δmudr1* transcripts in a sibling of the male parent of the SB03 family (SS79-21) did not reduce *mudrA* abundance compared with that in the sibling plant SS79-20, which did not inherit this deletion (or any other detectable deletion derivative). Stochastic epigenetic silencing of Mutator activity in SB03-9 plant is the most likely explanation for the decrease of both *mudrA* and *Δmudr1* transcript abundance in those plants (Bennetzen et al., 1993).

Second, transcripts from *ΔMuDR1* and *ΔMuDR 2* did not affect the methylation status of *Mu* TIRs. SB03 sibling plants were grown from kernels with different frequencies of *Mu* excision scored in the aleurone (Figure 4F). Decreased spotting frequency is an indicator of the incipient loss of Mutator activity, which is accompanied by methylation of the TIRs of *Mu* elements (Chandler and Walbot, 1986). HinfI cleaves unmethylated sites within the TIRs of *Mu1* and *Mu2* elements, resulting in 1.3- or 1.6-kb fragments, respectively. Because the HinfI sites are within the MURA transposase binding site defined in vitro (Benito and Walbot, 1997), lack of methylation is a molecular phenotype indicative of a transcriptionally and functionally active *MuDR*. We found that all SB03 plants retained unmethylated TIRs in the *Mu1* elements (Figure 4G), indicating that *MuDR* is active.

Third, *ΔMuDR1*, the older deletion derivative present in all SB03 plants, had low transcript levels in plants that also inherited *ΔMuDR2* (SB03-7, -10, and -11), with the exception of plant SB03-4. *Δmudr1* transcripts were detected easily in all plants that inherited only *ΔMuDR1*. Therefore, it appears that some deletion derivatives affect the transcript abundance of other deletion transcripts without influencing *MuDR* transcripts.

Generation and Characterization of Transgenic Plants Expressing Antisense *mudrA or* Antisense *mudrB* Transcripts

Nearly all somatic excision events of engineered *Mu1* (*RescueMu*) elements occur during or after the last cell division (Raizada et al., 2001c), similar to the very late excision observed in mutable alleles with *MuDR* and nonautonomous *Mu* insertions. We hypothesize that this late excision timing ensures that most internal deletions within *MuDR* also occur late in development. If this is true, then antisense transcripts produced so late in development may not influence *MuDR* activities in the soma, because *MuDR* transcripts and protein products already are present. Furthermore, the vast majority of somatic deletions are nontransmissible: only those *ΔMuDR* arising in lineages that enter meiosis can be transmitted to the next generation. Transcript analysis of

Table 3. Survey for Deleted *MuDR* (*ΔMuDR*) Elements in Active Mutator Plants

	F1 Family[a]												
Variable	T55	T57	T62	T63	T64	T56	T65	T69	SK26	SK30	SB03	SB36	Total
Number of *ΔMuDR*[b]	4/6[c]	2/3	1/2	4/6	2/3	0/0	1/1	2/3	2/5	0/3	0/4	2/6	20/42
Deletion of IGR[d]	1/2[e]	0/1	1/2	1/2	1/2	0/0	0/0	1/1	1/2	0/2	0/4	2/3	8/21
Plants carrying *ΔMuDR*	5/6[f]	12/12	4/4	6/6	6/6	0/6	1/6	5/10	12/12	11/11	11/11	4/16	77/106

[a] Mutator plants were crossed to/by anthocyanin tester lines to produce F1 progeny ears; the resulting F1 plants were screened for the presence of *ΔMuDR* elements using DNA blot hybridization.
[b] Genomic DNA was prepared from parents and sibling plants of each F1 family. SstI-digested genomic DNA was probed with a mixture of *mudrA* (A) and *mudrB* (B) fragments (see Figure 1A). Bands smaller than the 4.7-kb intact *MuDR* were scored as deleted *MuDR*.
[c] Number of new *ΔMuDR*/total number of *ΔMuDR* detected in the family. The total *ΔMuDR* count includes new (found in only one individual) and parental (segregating or present in all members of the family) deletions. Segregating parental bands of the identical size were considered to represent one deletion event that occurred in a previous generation.
[d] Blots used for the detection of *ΔMuDR* were reprobed with an intergenic region (IGR) DNA fragment (see Figure 1A). *ΔMuDR* bands that failed to hybridize were scored as deletions of the intergenic region. Intergenic region deletions of identical size were counted as one event.
[e] Number of new *ΔMuDR* elements that lack the intergenic region/total number of *ΔMuDR* in the family that lacks the intergenic region.
[f] Number of plants carrying a *ΔMuDR*/number of total plants examined.

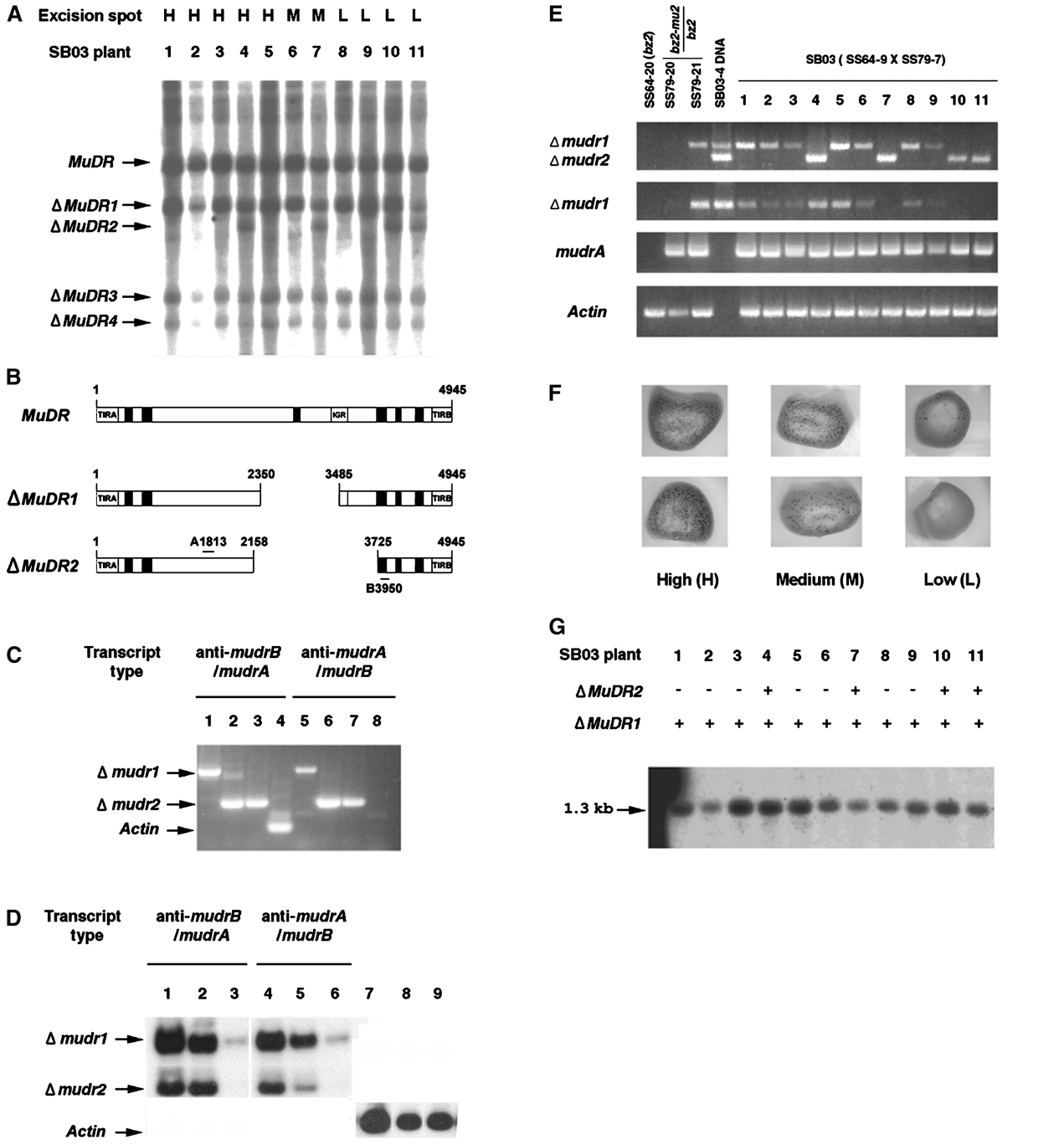

Figure 4. Molecular and Structural Analyses of Two Germinally Deleted *MuDR* Elements and Their Transcripts.

(A) Detection of heritable deleted *MuDR* derivatives in sibling plants grown from SB03. Genomic DNA was prepared from these plants, digested with SstI, and blotted and probed with the A and B probe described in Figure 1B. Four deleted elements (*ΔMuDR1* to *ΔMuDR4*) were found and are indicated with arrows. H, high; M, medium; L, low.

(B) Schemes of the intact *MuDR* and two *ΔMuDR* elements. Primers 3 and 12 shown in Figure 1A were used to amplify portions of *ΔMuDR1* and *ΔMuDR2*. The amplified fragments were sequenced to confirm the structures.

(C) Directional RT-PCR cloning of antisense *mudrB*/*mudrA* (anti-*mudrB*/*mudrA*) and antisense *mudrA*/*mudrB* (anti-*mudrA*/*mudrB*) from total RNA of plants SB03-1 (lanes 1 and 5), SB03-4 (lanes 2 and 6), and SB03-11 (lanes 3 and 7). Single-stranded cDNA was obtained using either primer 12 (lanes 1, 2, and 3) or primer 3 (lanes 5, 6, and 7). After removal of template RNA and inactivation of the reverse transcriptase, cDNA was amplified using primer 3 or primer 12, as appropriate. Control amplification of sense actin transcripts (lane 4), but not antisense transcripts (lane 8), confirmed that the RT-PCR was directional in this experiment. Data show RT-PCR products fractionated on a 1% agarose gel and stained with ethidium bromide.

(D) Amplification of the *Δmudr* transcripts from several RNA sources. Total RNA was extracted from plant SB03-4 and fractionated into poly(A^+) and poly(A^-) RNA as described in Methods. Directional RT-PCR was performed using total RNA (lanes 1, 4, and 7), poly(A^-) RNA (lanes 2, 5, and 8), or poly(A^+) RNA (lanes 3, 6, and 9) as described in **(C)**. The amplified RT-PCR products were fractionated on an agarose gel and detected using the A and B DNA probes after blotting on a nylon membrane. Sense actin transcripts were amplified as a control.

the two transmissible deleted *MuDR*, *ΔMuDR1* and *ΔMuDR2*, showed that the majority of these messages were not polyadenylated properly (Figure 4D). By contrast, substantial amounts of polyadenylated antisense messages were detected easily from a seedling leaf of a Mutator plant (Figure 1C, lane 4).

Transgenic plants constitutively expressing antisense *mudrA* or antisense *mudrB* were used to further analyze the impact of antisense RNA expression on the abundance of sense *MuDR* messages and Mutator somatic excision activities. First, the effectiveness of transiently expressed antisense transcripts, transcribed from different regions of the *MuDR* element, was tested in reducing corresponding sense transcripts in maize Black Mexican Sweet protoplasts (see Figure 5A for schemes of the fusion constructs and Table 4 for the transient analysis data). This study identified the most effective region of antisense *mudrA* (exon 4 and the 3′ UTR) and antisense *mudrB* (full-length antisense *mudrB* including the 3′ UTR and more than half of the 5′ UTR). We then generated transgenic maize expressing antisense *mudrA* (*pAA3*; *pAHC17*:*Anti-mudrA*) or antisense *mudrB* (*pABF*; *pAHC17*:*Anti-mudrB*) under the control of the maize *Ubiquitin1* (*Ubi1*) promoter.

Previous work established that a maize *Ubi1* promoter is highly active in most maize tissues, including roots, developing anthers, and pollen (Raizada et al., 2001a). We confirmed that *Ubi1* transcripts also are abundant in aleurone cells through 30 days after pollination (Figure 5B), when mitotic proliferation has finished and when most *Mu1* excisions have occurred (Levy and Walbot, 1990; Raizada and Walbot, 2000). Table 5 summarizes the genetic analysis and transgene expression of five independent antisense transgenic lines for each construct. In nearly all T0 plants and their T1 progeny, there was an excellent correspondence of herbicide resistance, which was used as the selection marker, and transgene expression: most herbicide-resistant T0 and T1 seedling plants expressed the corresponding transgene (41 of 43 plants tested). Furthermore, we detected no expression of the antisense transgene in plants sensitive to Basta (data not shown). Exceptionally, two plants derived from the *Anti-mudrB*-8 and -10 insertion events conferred resistance to the herbicide, but expression of the transgene could not be detected. Collectively, these results indicate that both the *Bar* gene and the antisense *mudrA* or antisense *mudrB* gene construct were transcriptionally active initially and had inserted at a linked locus. In general, transgene expression, determined by sensitivity to the Basta treatment, was relatively well maintained through several generations for plants carrying *Anti-mudrA* (moderate to good maintenance in *Anti-mudrA*-3, -4, -5, and -11 and poor maintenance in *Anti-mudrA*-12). By contrast, *Anti-mudrB* transgene expression was lost frequently (poor maintenance in *Anti-mudrB*-2, -8, and -10 and moderate to poor maintenance in *Anti-mudrB*-1 and -3). The biological significance of the frequent silencing of *Anti-mudrB* expression has yet to be examined.

Antisense *MuDR* Transgene Expression Does Not Affect *mudrA* and *mudrB* Transcript Levels or Mutator Somatic Excision Activity

We selected progeny from two independently transformed *Anti-mudrA* lines (HSA9 carrying *Anti-mudrA*-4 and HSA22 carrying *Anti-mudrA*-5) and two *Anti-mudrB* lines (HSA3 carrying *Anti-mudrB*-1 and HSA32 carrying *Anti-mudrB*-3) for detailed analysis. These transgenic lines maintained good expression of both the *Bar* gene and the transgene, with some examples of silencing in lines with *Anti-mudrB*-1 (Table 5). Nonetheless, HSA3 of the *Anti-mudrB*-1 transgenic line showed good expression of both genes.

From a program of genetic crosses, we found that antisense transgenes did not influence somatic excision frequency (Tables 6 and 7). For example, *Bz2* T0 plants carrying *Anti-mudrA*-4 or -5 were crossed with *bz2* testers. T1 Basta-resistant (*Bz2*/*bz2*) plants grown from purple kernels then were crossed by a *bz2-mu2* Mutator male plant to produce HSA9 (*Anti-mudrA*-4) and HSA22 (*Anti-mudrA*-5) ear families. Because the Mutator parent was homozygous for the *bz2-mu2* reporter allele, all T2 progeny ears should segregate 1:1 for purple:spotted bronze kernels, and half of each color class should contain the antisense transgene. At this stage, 40 to 60% of the kernels were spotted, indicating that there was no impact of the antisense construct on somatic excision activity. As is typical of *Mu*-induced mutable alleles, most excision sectors consisted of 1 to 16 cells in transgenic and nontransgenic plants, indicative of similar excision timing.

We tested for antisense transgene effects in the subsequent generation. A population of plants was grown from T2 spotted kernels, categorized for Basta resistance, and crossed again by *bz2* tester. We expected that individuals with a *bz2*-

(E) Transcripts of *ΔMuDR1* and *ΔMuDR2* and expression levels of sense *mudrA* transcripts. Transcripts were amplified from total RNA of SB03 plants, from two plants in the family of the male parent (SS79-20 and SS79-21), and from a plant in the family of the female parent (SS64-20). Primers 3 and 12 were used for the amplification of both *Δmudr1* and *Δmudr2* transcripts (top gel). RT-PCR with primers 4 and 12 produces only *Δmudr1* transcripts (second gel). Sense *mudrA* transcripts were amplified using primers 5 and 9 (third gel). Note that these primers can amplify two known *mudrA* transcripts, because intron 3 is spliced in only ~80% of the transcripts (Hershberger et al., 1995); in this experiment, most transcripts appear to be spliced, because the smaller 490-bp product is visualized prominently by ethidium bromide staining. The Actin gel (bottom) indicates that RT-PCR amplification was performed as a control to determine if equal amounts of RNA were used in the experiment. Portions of the *ΔMuDR1* and *ΔMuDR2* elements were amplified by PCR from genomic DNA of plant SB03-4 to use for a size comparison with the RT-PCR products (top two gels only; lane 4). The PCR amplification was for 31 cycles.

(F) Representative kernels of the SB03 ear (SS64-3 × SS79-7) were classified as high, medium, or low spotted. *Mu* excision from a mutable *bz2-mu2* allele restores a functional *Bz2* gene, and this is a visual indicator of somatic Mutator activity, which varied from high (>150 spots on a 2 mm × 2 mm aleurone area of the kernels) to medium (10 to 150 spots) to low (<10 spots).

(G) Analysis of the methylation status at HinfI sites within the MURA binding sites in the TIRs of *Mu1* and *Mu2* elements. Genomic DNA extracted from SB03 individuals was digested with HinfI, and the resulting DNA gel blot was probed with a *Mu1*/*Mu2*-specific probe (Raizada and Walbot, 2000). In this family, there were no *Mu2* elements; consequently, only the 1.3-kb fragment generated from *Mu1* was detected.

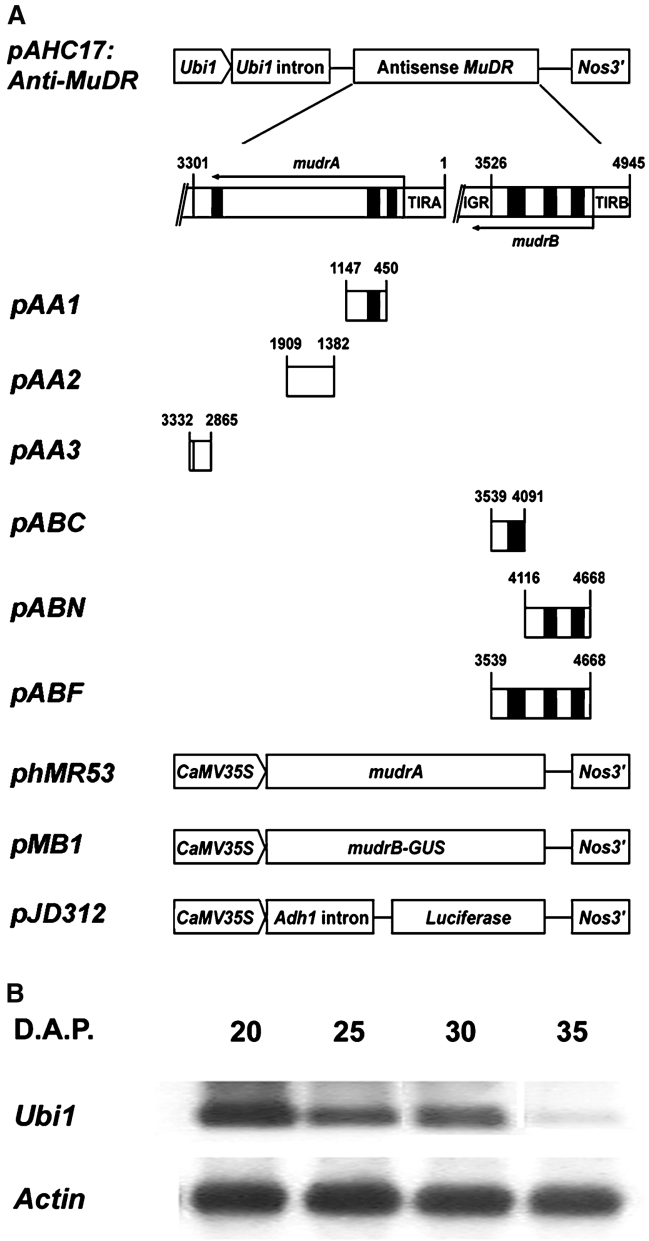

Figure 5. Promoter Constructs Used in Transient Gene Expression Analysis and *Ubi1* Expression in Developing Aleurone Layers.

(A) Schemes of constructs used in the experiments testing the effectiveness of antisense *MuDR* fragments in reducing corresponding sense transcript. PCR-amplified *MuDR* fragments were cloned into the 3′ region of *pAHC17* to make a transcriptional fusion with the DNA segment in an antisense orientation with respect to the ubiquitin promoter. Numbers on each PCR fragment represent the positions in *MuDR*. Drawings are not to scale. *CaMV*, *Cauliflower mosaic virus*; *Nos*, nopaline synthase.

(B) *Ubi1* expression in the aleurone layers of developing kernels. Total RNAs were prepared from aleurone layers of developing kernels at different days after pollination (D.A.P.). The RNAs were fractionated on a 1.2% agarose gel and probed with a *Ubi1*-specific oligonucleotide.

mu2/*bz2 Anti-mudrA*/− genotype would produce 25% spotted progeny kernels if the antisense transgene completely suppressed Mutator activity, whereas control plants lacking the transgene would produce 50% spotted kernel progeny. On a per ear basis, as shown in Table 6 for the lines examined with or without an antisense transgene, most ears fell into the 40 to 60% category, which is a frequency normally found in standard Mutator lines [78% of the progeny in the *Anti-mudrA*-4(+) family and 79% in the *Anti-mudrA*-5(+) family], and these were very similar to the sister lines lacking the transgene. On the other hand, 18% (12 of 68 ears) of *Anti-mudrA*-4(+) and 16% (12 of 76 ears) of *Anti-mudrA*-5(+) progeny ears produced T3 ears with <40% spotted kernels. Control families that did not contain the antisense *mudrA* transgene also gave similar results (17% in a line sister to *Anti-mudrA*-4 and 26% in a line sister to *Anti-mudrA*-5 progeny ears). Therefore, stochastic silencing is the best explanation for ears with <40% spotted kernels in the transgenic *Anti-mudrA*-4(+) and *Anti-mudrA*-5(+) lines.

On a per kernel basis, the expression of antisense *mudrA* also did not affect the frequency of *Mu1* somatic excisions (Table 7). In the control that did not carry *Anti-mudrA*, 65% of spotted kernels were classified as high spotted, 30.2% were classified as medium spotted, and 4.8% were classified as low spotted. Expression of an antisense *mudrA* transgene did not alter this distribution.

RT-PCR was used to determine whether expression of an antisense transgene reduced the abundance of the corresponding sense transcripts in T2 plants. *mudrA* and *mudrB* transcript levels are proportional to *MuDR* copy number in active Mutator lines (Rudenko and Walbot, 2001). Increasing amounts of *mudrA* and *mudrB* amplification from Mutator plants carrying higher *MuDR* copies (Figures 6A and 6B) support our idea that the RT-PCR in this experiment can be used to compare transcript levels between plants of one family. As a check for equal RNA samples, similar amounts of *mudrB* from plants were amplified from members of the HSA9 and HSA22 families in which an antisense *mudrA* locus is segregating (Figure 6A). Figures 6A and 6B show gene expression in representative T2 plants and the spotting phenotype of their resulting T3 ears for the *Anti-mudrA* and *Anti-mudrB* lines, respectively. Neither antisense *mudrA* nor antisense *mudrB* suppressed sense gene expression significantly compared with sibling plants without the transgene. Plants expressing antisense *mudrA* (HSA9-6, -8, -10, and -12 as well as HSA22-4, -5, -11, and -12) contained similar levels of *mudrA* transcripts compared with two control plants, HSA9-2 and HSA22-10, that lacked the transgene. Moreover, the frequency of excision per ear was similar in plants with the *Anti-mudrA* transgene and in the control plants. There were 40% spotted kernels in the ear of HSA9-6 × *bz2* tester and 48% in the ear of HSA22-12 × *bz2* compared with the control crosses, which had 55% in HSA9-2 × *bz2* and 45% in HSA22-10 × *bz2* (Figure 6A). Similarly, antisense *mudrB* transgenes had no quantitative impact on the expression of *mudrB* or the frequency of somatic excision in the T2 or T3 generation (Figure 6B, Table 6).

As a second check of RNA abundance, we examined the expression of *Anti-mudrA* and *mudrA* on an RNA gel blot (Figure 6C). Using an Anti-A fragment (Figure 1A) as a probe, we detected both endogenous *mudrA* (~2.8 kb) and *Anti-mudrA* (~600 bp) transcripts simultaneously on the same blot and compared the

Table 4. Transient Analysis of the Effectiveness of Antisense *MuDR* Fragments in Suppression of the Corresponding Sense Gene Expression in Maize Black Mexican Sweet Protoplasts

Construct[a]	Reporter Expression[b]	
	Comparison with *phMR53* (%)	Comparison with *pMB1* (%)
Antisense *mudrA*		
phMR53 only	100 ± 3.9	
phMR53 + *pABF* [3539 to 4668]	98 ± 5.8	
phMR53 + *pAA1* [1147 to 450]	90 ± 8.1	
phMR53 + *pAA2* [1909 to 1382]	94 ± 6.3	
phMR53 + *pAA3* [3332 to 2865]	78 ± 4.7	
Antisense *mudrB*		
pMB1 only		100 ± 4.5
pMB1 + *pAA3* [3332 to 2865]		98 ± 5.4
pMB1 + *pABF* [3539 to 4668]		70 ± 6.4
pMB1 + *pABN* [4116 to 4668]		96 ± 6.5
pMB1 + *pABC* [3539 to 4091]		106 ± 8.4

[a] Schemes of the constructs used in this experiment are shown in Figure 5A. The 5′ to 3′ positions of the antisense *MuDR* fragment in the *Ubi1*-driven expression vector are indicated in brackets.
[b] Expression data were normalized using luciferase expression derived from *pJD312*.

molar ratios of the transcripts. The T3 plants expressed antisense *mudrA* at 6.5 times (plant 11) to 20 times (plant 6) higher levels than endogenous *mudrA*. This massive expression of antisense RNA, however, did not affect the abundance of the sense transcripts significantly compared with that in sibling plants lacking the antisense transgene. All transgenic plants still expressed 80 to 120% of *mudrA* compared with a sibling control plant that does not carry the transgene (Figure 6C, plant 2). Similar results were found for antisense *mudrB* T3 plants (data not shown). About two-thirds of the transgene Anti-*mudrA* transcripts were polyadenylated, and slightly more than half of the total transgene transcripts were localized in the cytosol (Figure 6D, sec-

Table 5. Characterization of the Transgenic Lines Used in This Study

Genetic Locus	Cosegregation of the Transgene with Herbicide Resistance[a]		Transgene Segregation		Transgene/Herbicide Stability (Progression from T0 to T2)
	T0 Plant	T1 Seedling	T1 Plant	T2 Plant	
Anti-mudrA-3	3/3[b], medium[c]	3/3[d]	11 (40/120)[e,f]	N.D.[g]	Moderate to poor[h]
Anti-mudrA-4	3/3, weak	1/1	8 (34/75)	4 (24/54)[e,f]	Moderate to good
Anti-mudrA-5	3/3, weak	2/2	4 (29/59)	4 (24/54)	Good
Anti-mudrA-11	3/3, medium	1/1	8 (49/83)	1 (6/12)	Moderate to good
Anti-mudrA-12	3/3, medium	1/1	8 (28/73)	3 (1/41)	Poor
Anti-mudrB-1	3/3, medium	2/2	3 (30/39)	3 (12/35)	Moderate to poor
Anti-mudrB-2	3/3, weak	1/1	6 (29/83)	2 (2/28)	Poor
Anti-mudrB-3	3/3, weak	2/2	8 (43/65)	4 (20/45)	Moderate
Anti-mudrB-8	2/3, weak	N.D.	9 (15/88)	N.D.	Poor
Anti-mudrB-10	2/3, strong	N.D.	9 (4/79)	2 (0/35)	Poor

[a] Cosegregation (linkage) of transgene expression and herbicide resistance was evaluated by RNA gel blot analysis and a Basta sensitivity test, respectively, for the indicated samples.
[b] Number of plants expressing the transgene in the eighth leaf/number of Basta-resistant plants.
[c] Relative level of transgene expression determined by an RNA gel blot analysis. Assigning weak expression as 1.0, medium corresponds to fourfold to eightfold higher and strong corresponds to more than eight times higher expression than the weak level.
[d] Number of plants expressing the transgene in the fifth leaf/number of Basta-resistant plants.
[e] Number of ear families tested in each transgenic line (number of Basta-resistant plants/total plants tested). Data are the sum of results obtained from all families of that line. Transgenes were transmitted through the egg.
[f] Transgene expression was determined in families of plants by examining resistance to Basta applied to the tenth leaf.
[g] N.D., not determined.
[h] Families were ranked by the ratio of T1 or T2 plants expressing the transgene to those lacking it. Maintenance of ranges of the ratio from the T0 to the T2 generation was scored as good (1 ± 0.2), medium (1 ± 0.4), or poor (<0.5). A ratio <0.5 predicts a high probability of transgene silencing in the next generation.

Table 6. Effect of Antisense Transgene Expression on Somatic Excisions of *bz2-mu2*

	Number of Progeny Ears with Spotted Kernels within the Indicated Percentage[a]					
Genetic Locus (Female Parent)	10 to 20	21 to 29	30 to 39	40 to 60	>60 (%)	Total Ears
Anti-mudrA-4(−)[b]		4	8	56	4	72
Anti-mudrA-4(+)[b]	8		4	53	3	68
Anti-mudrA-5(−)	4		19	61	4	88
Anti-mudrA-5(+)			12	60	4	76
Anti-mudrB-1(−)			8	64		72
Anti-mudrB-1(+)				19		19
Anti-mudrB-3(−)		7	36	64	12	119
Anti-mudrB-3(+)			12	36		48

[a] T2 Mutator parents were tested for transgene expression as described in footnote b and were crossed by *bz2* testers to generate progeny ears. The percentage of spotted kernels in the resulting ears was calculated, and each ear was placed into a category as indicated.
[b] Transgene expression was determined in families of plants by examining resistance to Basta applied to the tenth leaf. (−), sensitive; (+), resistant.

ond gel from the top). Polyadenylation of the endogenous *mudrA* transcripts in the transgenic plants was less efficient compared with that of other transcripts, such as actin. By quantification of RNA gel blot intensities, we found a 10- to 12-fold molar excess of anti-*mudrA* transcripts compared with endogenous *mudrA* in both the cytoplasmic and nuclear fractions (Figure 6D, right gels); however, the abundance of total *mudrA* transcripts was unaffected (Figure 6C). We conclude that neither the abundance of *mudrA* and *mudrB* transcripts nor the somatic excision frequency or its timing is sensitive to the presence of a massive amount of antisense transcripts for these gene products in the nucleus and the cytosol of active Mutator plants.

DISCUSSION

Antisense transcripts can arise from active antisense promoters (Spicer and Sonenshein, 1992), from read-through transcription initiated from neighboring genes (Acheson, 1984), from transcription driven by an RNA-dependent RNA polymerase using small complementary RNAs or an inverted repeat transgene array as a primer (Cogoni and Macino, 1999), or from a gene transcription unit in *trans* (Lee et al., 1993). In this study, we demonstrate that chimeric sense/antisense transcripts of *MuDR* originate mainly from deletion derivatives of *MuDR* and not from read-through in an intact *MuDR* element. Antisense RNA structures and the absence of strong promoters within the *mudrA* or *mudrB* coding region suggest that transcription probably initiates normally at +162 in TIRB and at +168 in TIRA or the nearby second initiation site at +252.

Internal deletions that preferentially remove the 3′ UTR of *mudrA* and/or *mudrB*, including the intergenic region, either eliminate termination or polyadenylation signals or in some way prevent their use. As a consequence of frequent *MuDR* deletions and convergent transcription of the sense genes, these defective *MuDR* elements are prone to produce abundant chimeric sense/antisense transcripts that accumulate in active Mutator lines. Those antisense RNAs whose sequences are perfectly complementary to the endogenous sense RNA could interfere with sense RNA stability and translation or induce post-transcriptional gene silencing. We showed here, however, that the sense transcript abundances and Mutator activities are not obviously regulated by naturally occurring antisense RNAs. This lack of suppression also is evident in transgenic plants expressing massive amounts of antisense *mudr* transcripts, even when both sense and antisense transcripts are present in the same subcellular compartment. The antisense-expressing construct was proven to reduce the abundance of the corresponding sense transcripts in non-Mutator Black Mexican Sweet protoplasts over an ~24-h incubation (Table 4), but in intact plants there was no suppression effect; presumably, different conditions exist in situ in a Mutator plant carrying active *MuDR* elements than in the protoplasts of a non-Mutator line. Alternatively, the ratio of sense to antisense transcripts could differ in the electroporated protoplasts compared with intact plants containing an integrated transgene.

Structural Analysis of Antisense *MuDR* Transcripts

Only active Mutator plants produce antisense transcripts detectable by RNA gel blot hybridization analysis (Hershberger et al., 1995; Joanin et al., 1997). The origin of only one antisense

Table 7. Effect of Antisense *mudrA* Expression on the Frequency of *Mu1* Somatic Excision from *bz2-mu2*

	Excision Frequency		
Sample	High (>150[a])	Medium (10 to 150)	Low (<10)
Anti-mudrA (−)	65.0 ± 14.0[b]	30.2 ± 11.4	4.0 ± 3.2
Anti-mudrA (+)	66.4 ± 9.4	27.8 ± 8.1	5.8 ± 2.8

T3 progeny ears described in Table 6 were sampled from transgenic plants carrying *Anti-mudrA*-4 or *Anti-mudrA*-5.
[a] The number of excision spots in a 2 mm × 2 mm area was counted for each kernel using a Nikon stereo zoom microscope. Most excision sectors consist of 1 to 16 cells, and there was no significant difference in the excision timing depending on the expression of the transgene (data not shown).
[b] Spotted kernels were classified by their excision frequency as high, medium, and low. Numbers represent the percentage of kernels on each ear that belong to the indicated frequency category ± SD. Data were taken from counting of 1235 spotted kernels/8 ear families that do not express the transgene and of 1085 spotted kernels/7 ears families that express the antisense *mudrA* transgene.

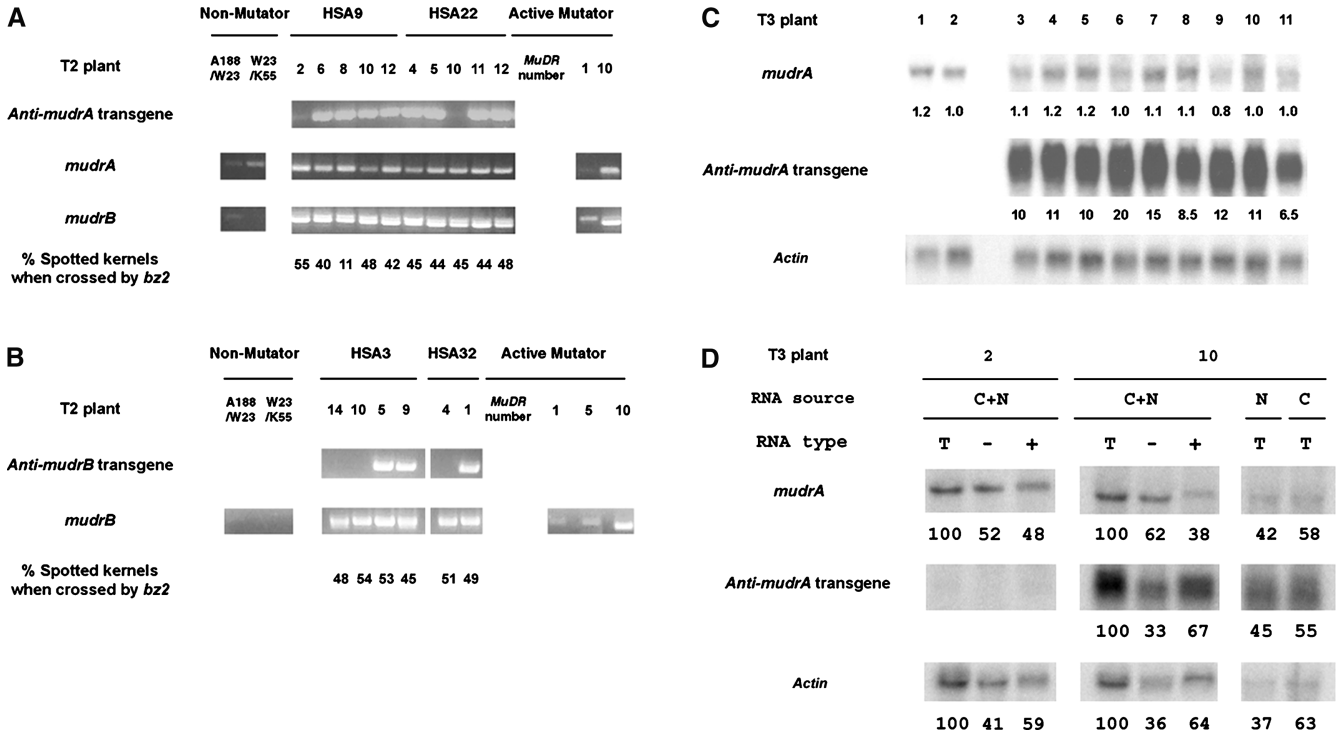

Figure 6. Molecular and Genetic Analyses of the Impact of Antisense Transgene Expression on *mudrA* and *mudrB* Transcript Abundance and on Somatic Excision Activity.

(A) and **(B)** Two transgenic families for each *Anti-mudrA* **(A)** or *Anti-mudrB* **(B)** were examined. These are T2 families generated by crossing to a *bz2-mu2* active Mutator line in a previous generation. RNA was extracted from transgenic plants and from individuals of two non-Mutator plants, the Hill hybrid (A188 × B73) used to make transgenic plants and W23 × K55 (*bz2* tester), and from active Mutator plants with varying numbers of *MuDR* elements (1, 5, or 10 copies). RT-PCR was performed to amplify antisense *mudrA* transcripts (using a primer residing in the nopaline synthase [*Nos*] 3′ region and primer 9), antisense *mudrB* transcripts (using the *Nos* 3′ primer and primer 8), endogenous *mudrA* transcripts (primers 5 and 9), and *mudrB* transcripts (primers 8 and 13). Two different splicing products were amplified for *mudrB*, as expected. Previously, data from RNase protection assays were used to estimate that *mudrB* retaining only the last intron (corresponding to the lower band in the bottom gel in **[A]**) represented 75% of total *mudrB* transcripts and that the transcript containing both introns 2 and 3 (corresponding to the upper band in **[A]**) represented 20% of the total RNA extracted from leaf samples of a high-copy *MuDR* line (Hershberger et al., 1995). PCR was performed for 31 cycles, and the amplified fragments were visualized by staining with ethidium bromide. Each transgenic individual (*bz2/bz2-mu2*) was crossed to the W23 × K55 *bz2* tester to allow the scoring of somatic excision spots in the progeny.

(C) Expression of antisense transgene and endogenous *mudrA* in T3 sibling plants. Total RNAs were prepared from seedlings of spotted sibling kernels of a T3 progeny ear (HSA22-12 × *bz2*). An RNA gel blot was probed with the Anti-A DNA fragment to detect the expression of the genes. The abundance of messages was quantified using a Kodak image analysis system as described in the Methods section, and they are normalized to the expression of actin. The numbers below each blot represent the relative abundance of messages compared with that of *mudrA* in plant 2. Plants 1 and 2 are control plants that do not carry the *Anti-mudrA* transgene.

(D) Polyadenylation and localization of transgenic anti-*mudrA* messages. Whole-plant total RNA (C+N), nuclear total RNA (N), or cytosolic total RNA (C) was isolated from leaves of plant 2 or plant 10 described in **(C)**. The whole-plant total RNA (T) was fractionated into poly(A$^-$) RNA (−) or poly(A$^+$) RNA (+), and the RNA preparations were separated on an agarose gel and then blotted on a nylon membrane. The abundance of messages probed with Anti-A DNA fragments was quantified as described in **(C)**. The numbers below each blot represent the percentages. For whole-plant RNA preparations (C+N), total RNA from the preparation was designated as 100%. The abundance of messages derived from the cytoplasmic or nuclear preparation is expressed as a fraction of the sum from both sources. Fifteen micrograms of total RNA or equivalent amounts of poly(A$^-$) RNA and poly(A$^+$) RNA or 10 μg of cytosolic RNA or the cell-volume equivalent amount of nuclear RNA (1 μg) were used for the RNA gel blot analysis (Alonso-Caplen et al., 1992).

transcript has been documented to date: a heritable deletion derivative (*d202*) missing 174 bp at the 3′ end of the *mudrA* gene encodes chimeric sense/antisense transcripts for both *mudrA* and *mudrB* (Lisch et al., 1999). However, this single transcript type does not account for the RNase protection results, indicating that many portions of *mudrA* and *mudrB* RNA are present in antisense form (Hershberger et al., 1995). In a multicopy *MuDR* plant, we identified diverse antisense transcripts and recovered 13 different chimeric transcripts from a small leaf disc of a single plant. These transcripts lacked 7 to 2909 bp of internal *MuDR* sequence, and none of the missing sequences occurred at points that match the consensus features of maize intron borders. We propose

that diverse somatic deletion derivatives arising during organ development are a major source of somatic antisense transcripts. Because we used RT-PCR primers residing within either *mudrA* or *mudrB*, *MuDR* elements deleted in the intergenic region may have been recovered preferentially. Thus, the antisense hybrid transcripts analyzed here could represent only a subset of antisense *MuDR* transcript diversity.

Germinal Deletions within *MuDR*

Plants with heritable *ΔMuDR* have provided fruitful genetic material to determine the roles of *mudrA* and *mudrB* in Mutator activities (Lisch et al., 1999). Despite their utility, the frequency of *MuDR* deletions has not been quantified. Analyzing families in which the immediate Mutator progenitors had several copies of *MuDR*, we found that 18.9% of progeny contained an independent, newly arising deletion derivative. Per element, the mutation frequency is $>10^{-2}$, many orders of magnitude greater than deletions within standard maize genes. In most cases, the *ΔMuDR* appeared to be multicopy, indicating that amplification, most likely by transposition, happened late in the life cycle of the previous generation. Considering only new deletions, 40% of the deletion events removed the intergenic region. This short 225-bp intergenic region and the neighboring sequences containing the 3′ UTRs of *mudrA* and *mudrB* were deleted preferentially. The intergenic region is composed of five distinct sets of direct repeats (11 to 27 bp in length) and three copies of one inverted repeat (12 bp in length) that can be modeled to fold into extended intrastrand duplexes (Hershberger et al., 1995). Removal of the intergenic region could affect the successful termination of *MuDR* transcription by changing DNA or RNA topology. The absence of the normal 3′ UTRs may result in a majority of the chimeric sense/antisense RNAs lacking polyadenylation.

Inability of Antisense *MuDR* Transcripts to Suppress *MuDR* Regulatory Elements and Mutator Activities

Although germinally transmitted *ΔMuDR* elements are transcriptionally active and produce chimeric sense/antisense transcripts, they have no measurable impact on *mudrA* transcript levels or *Mu1* TIR methylation. As determined by in situ hybridization, antisense *mudrA* transcripts colocalized with sense *mudrA* and *mudrB* transcripts in many tissues of active Mutator plants, and the sense and antisense transcripts may have been paired in vivo (Joanin et al., 1997).

As with documented cases of quelling in fungi, RNA interference in animals, and cosuppression in transgenic plants (reviewed by Matzke et al., 2001; Vance and Vaucheret, 2001), structural properties of *ΔMuDR* transcripts would be predicted to lead to RNA-based epigenetic gene silencing (Walbot and Rudenko, 2002). Ectopically expressed antisense RNAs are thought to pair with sense transcripts and feed into the double-stranded RNA–induced degradation pathway (Stam et al., 2000; Van Houdt et al., 2000; Serio et al., 2001), and in such cases, antisense transcripts can effectively silence homologous genes. Furthermore, the 3′ UTRs of *mudrA* and *mudrB* transcripts share repeat motifs that could fold into double-stranded structures (Hershberger et al., 1995). In recent studies, such intrastrand duplexes have been shown to be much more efficient than antisense RNAs in inducing homologous host gene silencing (Waterhouse et al., 1998; Chuang and Meyerowitz, 2000; Wesley et al., 2001).

Therefore, it is particularly interesting that sense transcripts and Mutator activities were not suppressed by either endogenous or transgene-encoded antisense *mudrA* and antisense *mudrB* RNA. In some previous studies assessing the impact of antisense transgenes, there was a lack of correlation between antisense and sense transcript abundance. For example, in antisense *chs* petunia transformants, Blokland et al. (1994) found no direct correlation between the presence of antisense RNA and *chs* suppression. A high level of antisense expression did not necessarily result in suppression of the corresponding endogenous gene, although *chs* silencing was the common outcome. Previously, in situ RNA analysis demonstrated that both sense and antisense *MuDR* transcripts were present in the same tissues and in the same cells (as in the endothelium, where both transcript types were present in all cells) (Joanin et al., 1997). In the present study, both sense and transgene-encoded antisense messages were detected in the nucleus and cytoplasm by RNA gel blot analysis, but we do not know whether the molar ratio of sense to antisense transcripts is similar in all cells. It is also unknown whether transcripts localized in the same compartment interact to form double-stranded RNA.

It is possible that antisense RNA has additional roles or fates beyond the formation of double-stranded RNA with sense transcripts. In that regard, we were interested in the observation that most *ΔMuDR1* and *ΔMuDR2* transcripts lack polyadenylation, a post-transcriptional modification required for efficient transport of mRNAs into the cytoplasm (Huang and Carmichael, 1996). If most *ΔMuDR* RNA is compartmentalized inside the nucleus, contact with properly processed *mudrA* and *mudrB* transcripts in the cytosol would be reduced, which might prevent chimeric sense/antisense transcripts from blocking the translation of the sense transcripts or triggering sense transcript degradation in that same subcellular location. A significant fraction of nuclear *MuDR* transcripts also were poly(A^-) RNA, particularly in lines undergoing silencing (Rudenko et al., 2003); hence, antisense poly(A^-) transcripts might act in that cellular compartment to disrupt sense transcript maturation. Molecular and genetic analysis using antisense transgenic plants, however, demonstrated that substantial antisense transcript accumulates in both the nucleus and the cytoplasm and that the antisense transcripts are present in greater than ~10-fold molar excess over the corresponding sense transcripts. Therefore, the tolerance of Mutator activities cannot be explained by the compartmentalization of the antisense transcripts.

Studies of antisense regulation in animals suggest two other mechanisms that might operate in *MuDR* regulation. X chromosome inactivation in mouse is initiated by an accumulation of *Xist* RNA; however, expression of the neighboring *Tsix* gene blocks this accumulation in a *cis*-limited manner. *Tsix* transcription starts 15 kb downstream of *Xist* and continues across the *Xist* locus, resulting in antisense RNA complementary to the *Xist* sense messages; the antisense transcripts effectively suppress *Xist* on that X chromosome but not on other ones (Lee et al., 1999; Stavropoulos et al., 2001). Such *cis* regulation seems unlikely to be effective for *MuDR*, because messages tran-

scribed from deleted elements would suppress only the sense transcripts encoded from the same deleted *MuDR* element. Transcripts originating from the dispersed *MuDR* elements in multicopy lines would be unaffected, although all copies of *MuDR* cease transcription during Mutator silencing (Hershberger et al., 1995). Alternatively, cosuppression of *Drosophila I* transposon activity by *I*-containing sense or antisense transgenes requires at least several and up to 10 generations to be established (Jensen et al., 1999). Thus, we cannot exclude the possibility that antisense repression of *MuDR* transposon activities requires many generations to establish the silenced state in these highly active Mutator plants.

Escape of *MuDR*/*Mu* from Maize Regulatory Mechanisms

DNA transposons are parasitic and mutagenic agents (Martienssen, 1998). They are hypothesized to increase the host's genetic diversity through transposition while ensuring their own propagation (Schwarz-Sommer et al., 1985). However, uncontrolled transposition, resulting in chromosomal instability or an excess of lethal alleles, could compromise host viability and thus end the relationship of each transposon with its host. Natural selection pressure should drive both partners to limit transposition but ensure transposon propagation, resulting in a spectrum of regulatory mechanisms. Two defensive features in maize plants limit these harmful effects of uncontrolled *MuDR*/*Mu* propagation: transposition is restricted to terminally differentiated cells, and coordinated epigenetic Mutator silencing occurs to quench the activities of multiple *MuDR* elements.

On the other hand, there are at least three examples of *MuDR* strategies by which the transposable element may evade several host defensive mechanisms. First, a subset of *hMuDR* elements escapes transcriptional downregulation during Mutator silencing (Rudenko and Walbot, 2001). Second, 21- to 26-nucleotide *MuDR*- or *hMuDR*-specific small RNAs are found in both non-Mutator and active or silencing Mutator plants, but their expression is not correlated with the epigenetic silencing of the element (Rudenko et al., 2003). This is particularly interesting because it is well known that transgenes expressing double-stranded RNA induce post-transcriptional gene silencing when coding sequences are used and induce transcriptional gene silencing when promoter sequences are used; small RNAs are thought to play a major role in both types of silencing phenomena (Sijen et al., 2001). Third, antisense transcripts resulting from the inevitable generation of frequent internal deletions do not affect *MuDR* transcript abundance and Mutator activities. In other words, *MuDR* is not suppressed by the homology-dependent gene silencing machinery of the host, at least that component of the mechanism triggered by antisense transcripts. Additionally, *ΔMuDR* elements are more likely to be silenced by chimeric transcripts than is an active *MuDR*. The deleted elements are coordinately silenced independently of transcription by intact *MuDR* elements. By contrast, active *MuDR* elements do not repress their own expression; rather, they enhance their own transcription and/or mRNA abundance (Raizada et al., 2001b).

We show here that antisense *MuDR* transcripts are not dominant-negative regulators of Mutator activities, but much remains to be learned before we fully understand the mechanism by which *MuDR* elements escape from antisense-mediated regulation. Detailed analysis of Mutator plants, such as investigation of whether specific endogenous or transgene-encoding antisense RNA types increase small RNA molecules in the plants or determination of whether a threshold level of the small molecules is needed to induce antisense-mediated negative regulation, may reveal important clues for understanding antisense-tolerant mechanisms of the *MuDR* elements.

METHODS

Plant Materials

All maize (*Zea mays*) Mutator stocks used were derived from lines originally supplied by D.S. Robertson (Iowa State University, Ames), including a line with the *a1-mum2* allele. *bz2* mutable alleles were recovered in our laboratory. Mutator lines have been maintained by selfing and by outcrossing to *bz2* or *a1* tester lines, as appropriate. The active Mutator lines SK26, SK30, SB03, and SB36 have a high number of *MuDR* elements (10 to 25 copies) and have the *bz2-mu2* mutable allele. They were crossed to a W23 *bz2* tester line in the previous generation. M857, M858, and M874 are active Mutator lines carrying several unmethylated, 4.9-kb *MuDR* elements and very few *Mu1*, *Mu2*, or *Mu3* elements; these lines were the gift of V.L. Chandler. Sibling plants of these lines were crossed to anthocyanin tester plants to produce progeny lines: M857 to *bz2* (T56 and T65), M858 to *bz2* (T55, T63, and T64), M858 to *c2* (T57), M858 to *r-g* tester (T62), and M874 to *bz1* (T69).

RNA Preparation, Reverse Transcription PCR Amplification, Subcloning, and Sequence Analysis of PCR Products

Total plant RNA and nuclear or cytoplasmic RNA preparations were isolated from 10 to 20 g of leaf tissue as described previously (Rudenko et al., 2003) using either RNeasy Maxi kits (Qiagen, Valencia, CA) or Trizol reagent (Invitrogen, Carlsbad, CA). Total RNA was fractionated into poly(A^+) and poly(A^-) RNA after determination of RNA concentration using an Oligotex mRNA Midi Kit (Qiagen) and then kept in the same volume of RNA storage buffer (Ambion, Austin, TX) as the initial total RNA sample. RNA preparations for reverse transcription (RT) PCR analysis were treated further with RNase-free DNase I (Gibco BRL, Gaithersburg, MD). For RT-PCR amplification of the antisense *mudrB* transcripts shown in Figure 1C, sense-strand cDNA was reverse-transcribed (OneStep RT-PCR kit; Qiagen) at 50°C for 30 min using the strand-specific primer B3843 (5′-TTCGAAGAGCACTCTCGTGTC-3′). Reverse-transcribed cDNA was amplified after adding the opposite strand-specific primer, A1621 (5′-CTTGCATCTGCTACTGGTGTAGATGGCC-3′). To amplify antisense *mudrA* transcripts, A1621 was used as the RT primer and B3843 was added for PCR amplification. Control reactions were preincubated with DNase-free RNase (Boehringer Mannheim, Indianapolis, IN) according to the manufacturer's protocol.

For the retrieval of polyadenylated antisense transcripts, amplification of the 3′ cDNA ends was performed from total RNA using a 5′/3′ rapid amplification of cDNA ends kit (Boehringer Mannheim) according to the manufacturer's instructions. In brief, reverse transcription was performed at 45°C using an oligo(dT)-anchored primer (5′-GACCACGCGTATCGATGTCGATTTTTTTTTTTTTTTT-3′). Antisense *mudrA* or antisense *mudrB* cDNA then was amplified using a PCR-anchor primer (5′-GACCACGCGTATCGATGTCGAC-3′) and strand-specific primers residing in different regions of the antisense strand of *mudrA* or *mudrB*. PCR fragments were gel-purified from the RT-PCR product and subcloned into pT-Adv; plasmids were transformed into *Escherichia coli* strain DH10B according to the supplier's protocol (Clontech, Palo Alto, CA). Double-strand cycle se-

quencing with Big-Dye terminators was performed at the Stanford University Protein and Nucleic Acid Biotechnology Facility.

The antisense cDNAs listed in Table 1 were amplified and cloned as described above but using the RT-PCR primer sets indicated in the same table. All RT-PCR procedures used OneStep RT-PCR (Qiagen) and were performed using DNase-treated RNA samples and the following primers: A493 (5′-TTCCCAACTCCCCCGATGTAG-3′), A1813 (5′-CCGTATGCTGAGAGAAGAGAATGC-3′), A2298 (5′-ATGACTAAACATGTCGTGAATGCAG-3′), A2713 (5′-TCTAGCTACAAGTGCCCTTTGAATGG-3′), A2907 (5′-TACAGCCAGACGTAGCAGAGG-3′), A2952 (5′-ATCCACAGCCAGAGACAGAACAATTGGG-3′), IGR3501 (5′-TATAACACACATGAATAACACTGAGCC-3′), A3276 (5′-GGGCTTGTTCTTAGCAGTCTTACAACC-3′), IGR3469 (5′-CAAGCAATCTGTTTCTCTGAACTGGGCG-3′), B3950 (5′-TCTAGATGATGATGAACTTGGTGATGGG-3′), B4334 (5′-CCATTGCCGTGGAGAAGGTTGAAGCAG-3′), B4473 (5′-ATTGTCCACCGAGCAAAGTGG-3′), and NOS3′ (5′-CCGGCAACAGGATTCAATCTTAAGAAAC-3′). The maize actin primers pMAcl 5′ and pMAcl 3′ (Raizada and Walbot, 2000) were added to the reactions as an internal RT-PCR and RNA quantity control. When RT-PCR products were analyzed using DNA gel blot analysis, 1 μL of RT-PCR product after 26 cycles of PCR amplification was separated by electrophoresis on a 1.0% agarose gel and visualized by standard DNA gel blot analysis using gene-specific probes as indicated in the legend of Figure 4D.

Genomic DNA Analysis

Plant genomic DNA was isolated using the DNeasy Plant Mini Kit (Qiagen) according to the manufacturer's instructions. DNA aliquots of 5 μg were digested with SstI or HinfI, fractionated by electrophoresis on 0.8% agarose gels, transferred to a Hybond N^+ membrane (Amersham Pharmacia Biotech, Piscataway, NJ), and probed with α-^{32}P-dCTP–labeled DNA fragments as indicated in the legends of Figures 1B, 4A, and 4G. Hybridization and washing of the membranes were performed as described previously (Warren and Hershberger, 1994).

RNA Gel Blot Analysis

Total RNA preparations were heat-denatured at 55°C for 15 min and fractionated on a 1.2% agarose gel containing formaldehyde. After transfer to a Hybond N^+ membrane, the membrane was probed with α-^{32}P-dCTP–labeled DNA probes and washed under the conditions described previously (Hershberger et al., 1995). When an oligonucleotide was used as a probe to detect the expression of *Ubi1*, a gene-specific oligonucleotide (5′-GCAGATACTTTGACAACC-3′) was end-labeled with α-^{32}P-dCTP and hybridization and washing were performed as described by Christensen et al. (1992).

Hybridization Probes

Transposon-specific double-stranded DNA probes A, B, and IGR were generated by PCR amplification from the *pMu9.6 MuDR* clone (Raizada and Walbot, 2000) using gene-specific primers. The *mudrA* probe (A) corresponds to *MuDR* positions 464 to 3276, the *mudrB* probe (B) corresponds to positions 3501 to 4495, the intergenic region probe (IGR) corresponds to positions 3297 to 3548, and the antisense *mudrA* probe (Anti-A) corresponds to positions 2865 to 3332. The *Mu1*/*Mu2*-specific probe and an actin probe were prepared as described by Raizada and Walbot (2000). Primer sets used for the *MuDR*-specific PCR amplifications were as follows: A (5′-CAGTTTCAATTCGCTAGACTCCAACGG-3′ and 5′-CTGGGCTTGTTCTTAGCAGTCTTACAACC-3′); B (5′-TATAACACACATGAATAACACTGAGCC-3′ and 5′-TTCTCTGCTCCTGTGCGGATGGATTG-3′); IGR (5′-CAGTTTTAGTTGCCAGTTCGTTGCTTCC-3′ and 5′-TATCTGTTTTGTGTTATATTTTATCT-3′); and Anti-A (5′-TTGGATCCCTAAAGAGCTTCGGACTTCTTC-3′ and 5′-ATGGATCCGAACCTGGAAGCAACGAACTGGC-3′).

Plasmid Construction

Plasmids were constructed using routine DNA manipulation protocols (Sambrook et al., 1989) and purified from bacterial cultures using Plasmid Max Prep Kits (Qiagen). The structures of the plasmid constructs are diagrammed in Figures 3 and 5A. Detailed descriptions for *pJB4*, *pJB12*, *pMB5* (Benito and Walbot, 1994), *pJD312* (Luehrsen et al., 1992), *pAHC17* (Christensen and Quail, 1996), *pBARGUS* (Fromm et al., 1990), *phMR53* (Raizada and Walbot, 2000), and *pMB1* (Ono et al., 2002) are available in the literature.

Antisense Promoter Construct

Regions of *MuDR* were amplified by PCR from *pMu9.6* (Raizada and Walbot, 2000) using the PstI- and KpnI-adapted primer sets listed below. The enzyme-digested PCR fragments were subcloned into *pJD312* digested with the same enzymes to replace the *Cauliflower mosaic virus* 35S promoter fragment of the luciferase expression plasmid with the *MuDR* fragment. The resulting constructs harbor a *MuDR* fragment followed by the first intron of the maize *Adh1* gene inserted upstream of the luciferase coding region. The primer sets used for the PCR construction of individual plasmids were as follows: (1) *pAP1* [4612 to 3307] (5′-CAGCTGCAGCGGCAATGCTGGACCGATTC-3′ and 5′-GTTGGTACCTTGCCAGTTCGTTGCTTCCC-3′); (2) *pAP2* [4292 to 2143] 5′-CAGCTGCAGGATTATACAAACTCATACACTC-3′ and 5′-CGAGGTACCCTGTTTCATCGTAGGCGAAGG-3′); (3) *pBP1* [445 to 1900] (5′-AAGCTGCAGGATCCATGGACTTGACGCCC-3′ and 5′-TAAGGTACCCTGCTGGATACATGTGCTCT-3′); (4) *pBP2* [2124 to 3540] (5′-CAGCTGCAGACAATGGAACTGTTTCATCG-3′ and 5′-TAAGGTACCTGTGTGTTATATGTTATCTG-3′); (5) *pBP3* [1212 to 2871] (5′-CACCTGCAGTGGAAGGAGGAGGACTACTAC-3′ and 5′-TAAGGTACCGGGATCCAATTTTTTGTGGTG-3′); and (6) *pBP4* [3297 to 3443] (5′-GGGCTGCAGTCAGTTTTAGTTGCCAGTTCG-3′ and 5′-AATGGTACCCGACAATTGCAAGCAATCTG-3′).

Antisense RNA Expression Construct

Regions of *mudrB* or *mudrA* were amplified from *pMu9.6* (Raizada and Walbot, 2000) by PCR using BamHI-adapted primer sets. The enzyme-digested PCR fragment was subcloned into *pAHC17* digested with the same enzyme. Bacterial clones harboring fusion plasmids, which result in the expression of antisense *mudrA* or antisense *mudrB* fragments directed by the maize *Ubi1* promoter, were selected. The primer sets used for the PCR construction of individual plasmid were as follows: (1) *pABN* [3539 to 4091] (5′-GACGGATCCATTAGTTCTTACAACCTC-3′ and 5′-CAAGGATCCCGGGTTTCTGGAACATGT-3′); (2) *pABC* [4116 to 4668] (5′-GTTGGATCCGAATGCAACAGTTTAG-3′ and 5′-CGCGGATCCTTGCGGTCTCCTCTTCTC-3′); (3) *pABF* [3539 to 4668] (5′-GACGGATCCATTAGTTCTTACAACCTC-3′ and 5′-CGCGGATCCTTGCGGTCTCCTCTTCTC-3′); (4) *pAA1* [450 to 1147] (5′-TTTGGATCCATGGACTTGACGCCCAG-3′ and 5′-CATGGATCCTCCACGGGCAATCACCAC-3′); (5) *pAA2* [1382 to 1909] (5′-GTAGGATCCTTGGGAGGAAAGCTTCCAG-3′ and 5′-GCTGGATCCATGTGCTCTGACCCAGCAT-3′); and (6) *pAA3* [2865 to 3332] (5′-TTGGATCCCTAAAGAGCTTCGGACTTCTTC-3′ and 5′-ATGGATCCGAACCTGGAAGCAACGAACTGGC-3′).

The restriction site in each primer is underlined. The portion of *MuDR* amplified is indicated in brackets using the numbering system of Hershberger et al. (1991). The proper orientations of gene fragments in the final fusion constructs were confirmed by cycle sequencing at the Stanford University Protein and Nucleic Acid Biotechnology Facility.

Transient Gene Expression Analysis

Preparation of maize Black Mexican Sweet protoplasts and electroporation and transient expression assays were performed as described previously (Carle-Urioste et al., 1995). For the experiment testing antisense promoter activity, 20 μg of each *MuDR* fragment fusion construct (*pAP1*or *pAP2* for antisense *mudrA* promoter activity and *pBP1*, *pBP2*, *pBP3*, or *pBP4* for antisense *mudrB* promoter activity) was electroporated into 10^6 Black Mexican Sweet protoplasts together with 10 μg of β-glucuronidase (GUS)–expressing *pJB4* plasmid. The transformed protoplasts then were collected after 24 h of incubation in growth medium, and the activity of GUS and luciferase in protoplast lysates was quantified as described previously (Carle-Urioste et al., 1995). GUS expression by *pJB4* was used as an internal transformation control; luciferase expression was normalized using the GUS expression for the data presented in Table 2. *pJB12* (*pJD312* without the *Cauliflower mosaic virus* 35S promoter) was used as a negative control, and *pMB5* (TIRB:*Adh1* intron:*LUC*) was used as a positive control. Luciferase activity was expressed as the number of photons emitted using luciferin during a 10-s integrative counting period. GUS activity was measured as picomoles of methylumbelliferone converted from methylumbelliferyl-β-D-glucuronide per minute.

For the experiment evaluating the effectiveness of antisense *MuDR* fragments, the impact of transiently expressed antisense transcripts in reducing the abundance of the corresponding sense messages was examined either by RNA gel blot analysis (for antisense *mudrA*) or by measurement of the expression from a MURB-GUS fusion protein (for antisense *mudrB*) (Ono et al., 2002). In brief, 20 μg of each antisense construct (*pAA1*, *pAA2*, or *pAA3* for antisense *mudrA* and *pABN*, *pABC*, or *pABF* for antisense *mudrB*) was electroporated into 10^6 Black Mexican Sweet protoplasts together with 10 μg of phMR53 and 10 μg of *pJD312* (for the antisense *mudrA* constructs) or 20 μg of *pMB1* and 10 μg of *pJD312* (for the antisense *mudrB* constructs). Antisense *mudrA*-transformed protoplasts were collected after 24 h of incubation in growth medium, and total RNA was isolated using Trizol reagent. The expression of sense *mudrA* was examined by RNA gel blot analysis using the *mudrA* fragment as a probe (Figure 1A), and the abundance of the transcript was quantified using a Kodak Digital Science Electrophoresis Documentation and Analysis System 120 and its 1D Image Analysis Software (Eastman Kodak, New Haven, CT). Antisense *mudrB*–transformed protoplasts were collected as described above, and the ratios of luciferase to GUS activities in protoplast lysates were quantified as described above. Luciferase expression by *pJD312* was used as an internal transformation control. The expression of *mudrA* transcript and MURB-GUS protein were normalized to luciferase units for the data presented in Table 4.

Transgenic Plants

The most effective antisense *mudrA* or antisense *mudrB* expression construct identified by the transient analysis, *pAA3* (*pAHC17:Anti-mudrA*) or *pABF* (*pAHC17:Anti-mudrB*), along with an herbicide selection plasmid (*pBARGUS*), was cobombarded into embryogenic Hill calli using biolistic delivery at the Plant Transformation Facility at Iowa State University (www.agron.iastate.edu/ptf/web/mainframe.htm/). The transformed calli were checked by RNA gel blot analysis for transgene expression and tested for resistance to 3 mg/mL bialaphos, the active ingredient in Basta herbicide (Spencer et al., 1990). The doubly positive calli were regenerated into T0 plants. Plants and progeny from five different transgenic calli for each antisense construct were chosen for detailed study. Herbicide resistance was used to identify transgene-expressing plants in the field or greenhouse because Basta resistance perfectly cosegregated with transgene expression (Table 5). Herbicide-resistant plants were identified as described previously (Raizada and Walbot, 2000).

The mature T0 plants were crossed to or by *bz2* or active Mutator lines with a high copy number of *MuDR* elements and homozygous for *bz2-mu2* (Hershberger et al., 1995). Because the T0 plants were *A1 Bz2 r-g/r-r*, it was not possible to score somatic excision immediately in T1 progeny by crossing to these Mutator lines; all kernels were purple or mottled and *Bz2/bz2-mu2*. Somatic excision in T2 kernels was scored after herbicide-resistant T1 plants were crossed to/by *bz2* (if they had been crossed to a Mutator line in the previous generation) or to/by an appropriate Mutator line (if they had been crossed to a non-Mutator tester in the previous generation) to generate a recessive background at *bz2*. In the T2 generation, half of the kernels on each ear were purple, and the other half of the kernels were scored for somatic excision of the segregating reporter allele. Progeny from spotted kernels in the T2 generation were tested further for Basta resistance and crossed again by *bz2* tester to score the somatic excision on kernels. Phenotypic comparisons were made to highly active Mutator plants carrying the *bz2-mu2* allele without an antisense transgene.

Upon request, materials integral to the findings presented in this publication will be made available in a timely manner to all investigators on similar terms for noncommercial research purposes. To obtain materials, please contact Virginia Walbot, walbot@stanford.edu.

ACKNOWLEDGMENTS

We are especially grateful to Akemi Ono, who generously provided the genomic blots, and to Vicki L. Chandler (University of Arizona, Tucson), who provided lines M874, M865, M858, and M857 used in the experiment described in Table 3. We thank M. Raizada, G. Rudenko, S. Shaw, G. Nan, D. Goodman, M. Fitzgerald, and S. Shah for stimulating discussions, critical reading, and thoughtful comments on the manuscript. We appreciate T. DeHoog and M. Abreu for their field and laboratory assistance. This research was supported by a grant from the National Institutes of Health (GM49681).

Received June 11, 2003; accepted August 13, 2003.

REFERENCES

Acheson, N.H. (1984). Kinetics and efficiency of polyadenylation of late polyomavirus nuclear-RNA: Generation of oligomeric polyadenylated RNAs and their processing into messenger RNA. Mol. Cell. Biol. **4,** 722–729.

Alonso-Caplen, F.V., Nemeroff, M.E., Qiu, Y., and Krug, R.M. (1992). Nucleocytoplasmic transport: The influenza virus NS1 protein regulates the transport of spliced NS2 mRNA and its precursor NS1 mRNA. Genes Dev. **6,** 255–267.

Benito, M.I., and Walbot, V. (1994). The terminal inverted repeat sequences of *MuDR* are functionally active promoters in maize cells. Maydica **39,** 255–264.

Benito, M.I., and Walbot, V. (1997). Characterization of the *Mutator* transposable element MURA transposase as a DNA-binding protein. Mol. Cell. Biol. **17,** 5165–5175.

Bennetzen, J.L., Springer, P.S., Cresse, A.D., and Hendrickx, M. (1993). Specificity and regulation of the Mutator transposable element system in maize. Crit. Rev. Plant Sci. **12,** 57–95.

Bisseling, T. (1999). The role of plant peptides in intercellular signaling. Curr. Opin. Plant Biol. **2,** 365–368.

Blokland, R., Geest, N., Mol, J.N.M., and Kooter, J.M. (1994). Transgene-mediated suppression of chalcone synthase expression in *Petunia hybrida* results from an increase in RNA turnover. Plant J. **6,** 861–877.

Bourque, J.E. (1995). Antisense strategies for genetic manipulations in plants. Plant Sci. **105,** 125–149.

Brendel, V., Kleffe, J., Carle-Urioste, J.C., and Walbot, V. (1998). Prediction of splice sites in plant pre-mRNA from sequence properties. J. Mol. Biol. **276,** 85–104.

Carle-Urioste, J.C., Marrs, K., Bodeau, J., and Walbot, V. (1995). Gene transfer to protoplasts: Transient gene expression analysis. In Gene Transfer to Plants, I. Potrykus and G. Spangenberg, eds (New York: Springer-Verlag), pp. 106–111.

Chandler, V.L., and Walbot, V. (1986). DNA modification of a maize transposable element correlates with loss of activity. Proc. Natl. Acad. Sci. USA **83,** 1767–1771.

Christensen, A.H., and Quail, P.H. (1996). Ubiquitin promoter-based vectors for high-level expression of selectable and/or screenable marker genes in monocotyledonous plants. Transgenic Res. **5,** 213–218.

Christensen, A.H., Sharrock, R.A., and Quail, P.H. (1992). Maize polyubiquitin genes: Structure, thermal perturbation of expression and transcript splicing, and promoter activity following transfer to protoplasts by electroporation. Plant Mol. Biol. **18,** 675–689.

Chuang, C.-F., and Meyerowitz, E.M. (2000). Specific and heritable genetic interference by double-stranded RNA in *Arabidopsis thaliana*. Proc. Natl. Acad. Sci. USA **97,** 4985–4990.

Cogoni, C., and Macino, G. (1999). Gene silencing in *Neurospora crassa* requires a protein homologous to RNA-dependent RNA polymerase. Nature **399,** 166–169.

Eisen, J.A., Benito, M.I., and Walbot, V. (1994). Sequence similarity of putative transposases links the maize *Mutator* autonomous element and a group of bacterial insertion sequences. Nucleic Acids Res. **22,** 2634–2636.

Fromm, M.E., Morrish, F., Armstrong, C., Williams, R., Thomas, J., and Klein, T.M. (1990). Inheritance and expression of chimeric genes in the progeny of transgenic maize plants. Bio/Technology **8,** 833–839.

Hershberger, R.J., Benito, M.-I., Hardeman, K.J., Warren, C., Chandler, V.L., and Walbot, V. (1995). Characterization of the major transcripts encoded by the regulator *MuDR* transposable element of maize. Genetics **140,** 1087–1098.

Hershberger, R.J., Warren, C.A., and Walbot, V. (1991). Mutator activity in maize correlates with the presence and expression of the *Mu* transposable element *Mu9*. Proc. Natl. Acad. Sci. USA **88,** 10198–10202.

Hsia, A.-P., and Schnable, P.S. (1996). DNA sequence analyses support the role of interrupted gap repair in the origin of internal deletions of the maize transposon *MuDR*. Genetics **142,** 603–618.

Huang, Y.Q., and Carmichael, G.G. (1996). Role of polyadenylation in nucleocytoplasmic transport of mRNA. Mol. Cell. Biol. **16,** 1534–1542.

Jensen, S., Gassama, M.-P., and Heidmann, T. (1999). Cosuppression of *I* transposon activity in Drosophila by *I*-containing sense and antisense transgenes. Genetics **153,** 1767–1774.

Joanin, P.J., Hershberger, R.J., Benito, M.J., and Walbot, V. (1997). Sense and antisense transcripts of the maize *MuDR* regulatory transposon localized by *in situ* hybridization. Plant Mol. Biol. **33,** 23–36.

Knee, R., Li, A.W., and Murphy, P.R. (1997). Characterization and tissue-specific expression of the rat basic fibroblast growth factor antisense mRNA and protein. Proc. Natl. Acad. Sci. USA **94,** 4943–4947.

Lankenau, S., Corces, V.G., and Lankenau, D.H. (1994). The *Drosophila micropia* retrotransposon encodes a testis-specific antisense RNA complementary to reverse transcriptase. Mol. Cell. Biol. **14,** 1764–1775.

Lee, J.T., Davidow, L.S., and Warshawsly, D. (1999). *Tsix*, a gene antisense to *Xist* at the X-inactivation center. Nat. Genet. **21,** 400–404.

Lee, R.C., Feinbaum, R.L., and Ambros, V. (1993). The *C. elegans* heterochronic gene *lin-4* encodes small RNAs with antisense complementarity to *lin-14*. Cell **75,** 843–854.

Levy, A.A., and Walbot, V. (1990). Regulation of the timing of transposable element excision during maize development. Science **248,** 1534–1537.

Lisch, D. (2002). *Mutator* transposons. Trends Plant Sci. **7,** 498–504.

Lisch, D., Carey, C.C., Dorweiler, J.E., and Chandler, V.L. (2002). A mutation that prevents paramutation in maize also reverses *Mutator* transposon methylation and silencing. Proc. Natl. Acad. Sci. USA **99,** 6130–6135.

Lisch, D., Girard, L., Donlin, M., and Freeling, M. (1999). Functional analysis of deletion derivatives of the maize transposon *MuDR* delineates roles for the MURA and MURB proteins. Genetics **151,** 331–341.

Luehrsen, K.R., Dewet, J.R., and Walbot, V. (1992). Transient expression analysis in plants using firefly luciferase reporter gene. Methods Enzymol. **216,** 397–414.

Martienssen, R. (1998). Transposons, DNA methylation and gene control. Trends Genet. **14,** 263–264.

Martienssen, R., and Baron, A. (1994). Coordinate suppression of mutations caused by Robertson's *Mutator* transposons in maize. Genetics **136,** 1157–1170.

Matzke, M.A., Matzke, A.J.M., Pruss, G.J., and Vance, V.B. (2001). RNA-based silencing strategies in plants. Curr. Opin. Genet. Dev. **11,** 221–227.

Ono, A., Kim, S.-H., and Walbot, V. (2002). Subcellular localization of MURA and MURB proteins encoded by the maize *MuDR* transposon. Plant Mol. Biol. **50,** 599–611.

Raizada, M.N., Benito, M.-I., and Walbot, V. (2001a). The *MuDR* transposon terminal inverted repeat contains a complex plant promoter directing distinct somatic and germinal programs. Plant J. **25,** 79–91.

Raizada, M.N., Brewer, K.V., and Walbot, V. (2001b). A maize *MuDR* transposon promoter shows limited autoregulation. Mol. Gen. Genomics **265,** 82–94.

Raizada, M.N., Nan, G.-L., and Walbot, V. (2001c). Somatic and germinal mobility of the *RescueMu* transposon in transgenic maize. Plant Cell **13,** 1587–1608.

Raizada, M.N., and Walbot, V. (2000). The late developmental pattern of *Mu* transposon excision is conferred by a cauliflower mosaic virus 35S-driven MURA cDNA in transgenic maize. Plant Cell **12,** 5–21.

Rudenko, G.N., Ono, A., and Walbot, V. (2003). Initiation of silencing of maize *MuDR*/*Mu* transposable elements. Plant J. **33,** 1013–1025.

Rudenko, G.N., and Walbot, V. (2001). Expression and post-transcriptional regulation of maize transposable element *MuDR* and its derivatives. Plant Cell **13,** 553–570.

Sambrook, J., Fritsch, E.F., and Maniatis, T. (1989). Molecular Cloning: A Laboratory Manual. (Cold Spring Harbor, NY: Cold Spring Harbor Laboratory Press).

Schwarz-Sommer, Z.A., Gierl, A., Cuypers, H., Peterson, P.A., and Saedler, H. (1985). Plant transposable elements generate the DNA sequence diversity needed in evolution. EMBO J. **4,** 591–597.

Serio, F.D., Schob, H., Iglesias, A., Tarina, C., Bouldoires, E., and Meins, F., Jr. (2001). Sense- and antisense-mediated gene silencing in tobacco is inhibited by the same viral suppressors and is associated with accumulation of small RNAs. Proc. Natl. Acad. Sci. USA **98,** 6506–6510.

Sijen, T., Vijn, I., Rebocho, A., van Blokland, R., Roelofs, D., Mol, J.N.M., and Kooter, J.M. (2001). Transcriptional and posttranscriptional gene silencing are mechanistically related. Curr. Biol. **11,** 436–440.

Simons, R.W., and Kleckner, N. (1988). Biological regulation by antisense RNA in prokaryotes. Annu. Rev. Genet. **22,** 567–600.

Spencer, T.M., Gordon-Kamm, W.J., Daines, R.J., Start, W.G., and Lemaux, P.G. (1990). Bialaphos selection of stable transformants from maize cell culture. Theor. Appl. Genet. **2,** 111–126.

Spicer, D.B., and Sonenshein, G.E. (1992). An antisense promoter of the murine *c-myc* gene is localized within intron 2. Mol. Cell. Biol. **12,** 1324–1329.

Stam, M., Bruin, R., Blokland, R., Hoorn, R.A.L., and Mol, J.N.M. (2000). Distinct features of post-transcriptional gene silencing by antisense transgenes in single copy and inverted T-DNA repeat loci. Plant J. **21,** 27–42.

Stavropoulos, N., Lu, N., and Lee, J.T. (2001). A functional role for *Tsix* transcription in blocking *Xist* RNA accumulation but not in X-chromosome choice. Proc. Natl. Acad. Sci. USA **98,** 10232–10237.

Terryn, N., and Rouze, P. (2000). The sense of naturally transcribed antisense RNAs in plants. Trends Plant Sci. **5,** 394–396.

Vance, V., and Vaucheret, H. (2001). RNA silencing in plants: Defense and counterdefense. Science **292,** 2277–2280.

Van Houdt, H., Van Montagu, M., and Depicker, A. (2000). Both sense and antisense RNAs are targets for the sense transgene-induced posttranscriptional silencing mechanisms. Mol. Gen. Genet. **263,** 995–1002.

Walbot, V. (1986). Inheritance of *Mutator* activity in *Zea mays* as assayed by somatic instability of the *bz2-mu1* allele. Genetics **114,** 1293–1312.

Walbot, V. (1992). Strategies for mutagenesis and gene cloning using transposon tagging and T-DNA insertional mutagenesis. Annu. Rev. Plant Physiol. Plant Mol. Biol. **43,** 49–82.

Walbot, V., and Rudenko, G.N. (2002). *MuDR*/*Mu* transposable elements of maize. In Mobile DNA II, N.L. Craig, R. Craigie, M. Gellert, and A. Lambowitz, eds (Washington, DC: American Society of Microbiology), pp. 533–564.

Warren, C.A., and Hershberger, R.J. (1994). Southern blots of maize genomic DNA. In The Maize Handbook, M. Freeling and V. Walbot, eds (New York: Springer-Verlag), pp. 566–568.

Waterhouse, P.M., Graham, M.W., and Wang, M.-B. (1998). Virus resistance and gene silencing in plants can be induced by simultaneous expression of sense and antisense RNA. Proc. Natl. Acad. Sci. USA **95,** 13959–13964.

Waterhouse, P.M., Wang, M.-B., and Finnegan, E.J. (2001). Role of short RNAs in gene silencing. Trends Plant Sci. **6,** 297–301.

Wesley, S.V., et al. (2001). Construct design for efficient, effective and high-throughput gene silencing in plants. Plant J. **27,** 581–590.

The Plant Cell